EUROPEAN COMMISSION
5th EURATOM FRAMEWORK PROGRAMME 1998-2002
KEY ACTION : NUCLEAR FISSION

HTR-E

High-Temperature Reactor Components and Systems

CONTRACT N°
FIKI-CT-2001-00177

HTR-E WP6 – Recommendation for helium specification

F. CELLIER/D. KACZOROWSKI

FRAMATOME ANP

FRANCE

Dissemination level : RE
Document N°: HTR-E-04/03-D-6-2-3
Status : Preliminary

FRAMATOME ANP

NOVATOME

NUMERO D'OTP OU EOTP	NOMBRE DE PAGES : 50 NOMBRE D'ANNEXES : 2	RAISON SOCIALE FOURNISSEUR :	
12.DTHTREW6NV	CONFIDENTIALITE : N	NUMERO DE COMMANDE	IMMATRICULATION FOURNISSEUR

CODE		DESIGNATION
AFFAIRE	H T	HTR
NATURE	D T	**Note Technique**
THEME		
MATERIEL		

TITRE : **HTR E WP 6 - Recommendation for helium specification**

TITRE ABREGE : **H T R E W P 6 - H E L I U M S P E C I F I C A T I O N**

IND	DATE	ETAT	REDACTEUR NOM-VISA	VERIFICATEUR NOM-VISA	APPROBATEUR NOM-VISA	MODIFICATIONS – OBSERVATIONS – ACCORDS REFERENCES ET DATES
A	08/03/2004	PRE	F. Cellier / D. Kaczorowski	P. Combrade	J. Roleau	First issue

IMMATRICULATION CLIENT :

IMMATRICULATION INTERNE : PVEK | DC | 04 | 0084 | ELR / [ ]

UNITE TYPE ANNEE CHRONO TRIGRAMMES

10, rue Juliette Récamier 69456 LYON CEDEX 06 - Téléphone : 04.72.74.82.21 - Télécopie : 04.72.74.84.90

Modifications

Revision	Date	Modifications
A	08/03/2004	First issue

Summary

This document contributes to HTR-E project WP6 (helium purification system) of the 5th European FWP. It is FRA-ANP contribution to deliverable D45.

The corrosion of metallic materials in impure helium environment appears to be a key factor for the development of a direct-cycle HTR, to which collapse mechanisms and service life of components and structures are closely related.

A review of material damages in former helium atmospheres has been performed. Due to the lack of experimental data for current candidate metallic material in helium environments at high temperature, and taking into account the work performed in 2002, a parametric study has been done using thermo dynamical phase stability diagrams.

Former HTR environments have been located on these phase stability diagrams in order to evaluate the surface reactions that can occur on the surface of a Ni-base alloy exposed to HTR helium at high temperature and the different domains of predominance of these surface reactions.

Based on this analysis, helium impurity concentration limits to maintain in the primary circuit, depending on the high-temperature range and with regard to the material aspects, are then recommended.

To summarize, safe behaviour of chromia forming Ni-base alloys in HTR helium requires at least three conditions dependent on the temperature and Cr activity in the alloy:

- P_{H2O}/P_{H2} > critical value to allow the formation of a protective oxide layer
- P_{CO} > critical value to avoid the microclimate reaction
- P_{CH4}/P_{H2O} < critical value to avoid the carburization and oxide reduction by the methane

Assuming values of surface Cr activities of about 0,3 under a protective oxide layer, order of magnitudes of the critical values to be specified for a safe behaviour of Ni-base alloy can be derived as follows:

- at 950° C, $P_{O2} > 2.\ 10^{-23}$, i.e. P_{H2O}/P_{H2} > a few 10^{-4} and P_{CO} > 150 µbar
- at 1000° C, $P_{O2} > 10^{-21}$, i.e.P_{H2O}/P_{H2} > a few 10^{-4} and P_{CO} > 450 µbar

It is noticeable that former helium compositions that are safe at relatively low temperatures (typically < 850 °C/900 °C) may not be safe at higher temperatures. Moreover, higher the temperature, faster the kinetics of material degradation. Thus, higher the temperature, more strict must be the enforcement of the above helium specifications.

This imply that, for modern HTR working at very high temperatures (typically above 850 °C/900 °C), the management of the impurities of the helium cannot be based on a simple purification

process which tends to remove all impurities from the environments without discrimination. In fact, some form of helium impurity control is required.

The target values of controlled impurity levels have to take into account the theoretical critical values presented above with additional safety margin to be evaluated from the variation of the operating parameters and the long term evolution of surface composition.

This work also shows that the precise determination of the helium specification requires more work in areas such as modelling the Cr activity of the alloys and its evolution on the alloy surfaces with time, constraints related to the oxidation of graphite at high temperature and the possible formation of C dust and CO_2 in the low temperature regions, and evaluation of the need for N_2 specification.

Regarding the characterization of the behaviour of Ni-base alloys in HTR, there is a significant lack of experimental data for high-temperature metallic material in impure helium environments. Complementary studies are still required on those materials particularly to establish their maximum temperature of use, including surface film evaporation at high temperature, and possible break away leading to surface oxide spallation.

Finally, possible deleterious nitriding effects at high temperature should be evaluated as well as the possible degradation by erosion by dusts present in the environment.

Contents

List of tables

List of figures

List of appendices

List of references

(1) HTR E WP6 Helium Purification
Nissen H.F.
Work plan HTR -E- 02/03-D-6 -0 -1 rev. A

(2) Review of the gas/Ni-base alloys interactions in HTR impure helium
Combrade P.
HTR -E- 02/09-D-6 -1 -2 rev. A

(3) German structural design rules for metallic HTR-components
Nickel H.
Proc. of first international spring school & symposium on advances in materials science (SAMS 94), KFA Juelich, 15-20 March 1994, pp 17-31

(4) Thermal stability and environmental compatibility of alloy 617.
Kimball, O.F
High temperature metallic materials for gas-cooled reactors. Proceedings of a specialists meeting held in Cracow, 20-23 June 1988

(5) Corrosion of High Temperature Alloys in the Primary Circuit Helium of High Temperature Gas Cooled Reactors - Part I: Theoretical Background
Quadakkers W.J. and Schuster H.
Werkstoffe und Korrosion, 36 (1985) p. 141

(6) Corrosion Mechanism of Nickel Base Alloys in the Primary Cooling Gas of High Temperature Reactors
Quadakkers W.J. and H. Schuster
Int. Congress Metal. Corr., 1984, Toronto

(7) Review of the Gas/Metal Interactions in HTR Helium up to 950° C
Menken G. et al.
Proc. Conf. Gas-Cooled Reactors Today, 1982, Bristol, UK, BNES

(8) High temperature corrosion in impure helium environments
Graham L.W.
High Temperature Technology 3, vol. 1 (1985) p. 3

(9) Review on high temperature gaseous corrosion and mechanical performance in carburizing and oxiding environments
Grabke H.J. and A. Schnaas
Proc. International Conference on Alloy 800, 1978, Petten.

(10) The effects of high-temperature reactor service environments on the mechanical properties of constructional alloys
Ennis, J.P. and H. Schuster
Proc. Conf. Gas-Cooled Reactors Today, 1982, Bristol, BNES

(11) Interaction of Metals with Primary Coolant Impurities: Comparison of Steam-Cycle and Advanced HTGRs
Jonhson W.R., Lai J.Y.
Specialists' meeting on high temperature metallic materials for application in gas-cooled reactors. Vienna, Austria. 4 – 6 May 1981 ; IWGGCR--4 pp J1-J22

(12) The development and application of a unified corrosion model for high-temperature gas-cooled reactor systems
Brenner K.G.E. and Graham L.W.
Nucl Technol., 66 vol. 2 (1984.) p. 404

(13) Comparison of mechanical and corrosion behaviour of alloy 800 H and the alloy AC66.
Pelz W., Weber H.
High temperature metallic materials for gas-cooled reactors. Proceedings of a specialists meeting held in Cracow, 20-23 June 1988 pp 176-183

(14) Qualification of metallic materials for application in advanced high temperature gas cooled reactors
Nickel H. et al.
Nucl. Technol., 58 (1982) p. 90

(15) Fundamental aspects of the interactions of HTR helium with metals and alloys
Pierce R.J., Huddle R.A.U., Kofstad P.
Dragon Project - paper N° 13 presented at the Metals Information Meeting, 1973, London

(16) Evaporation behavior of Hastelloy X alloys in simulated very high temperature reactor environments
Shindo M. and Kondo T.
Nucl. Technol. 66 vol. 2 (1984) p. 429

(17) Studies on improving the compatibility of nickel-base alloys with a High-Temperature Helium-Cooled Reactor (VHTR) environment
Proc. Conf. Gas-Cooled Reactors Today, 1982, Bristol, BNES

(18) Rapid decarburization and carburization in high temperature alloys in impure helium environments
Warren M.R., High Temperature Technology, 4, vol. 3 (1986) p. 119-130

(19) Corrosion of Metallic Materials in HTR-Helium Environments
Graham L.W
J. of Nuclear Materials 171 (1990) pp 76-83

(20) Thermodynamic and kinetic aspects of the corrosion of High-Temperature Alloys in High-Temperature Gas-Cooled Reactor helium
Quadakkers W.J. and Schuster H.
Nucl. Technol. 66, vol. 2 (1984) p. 383.

(21) A Unified Model for Metallic Corrosion IN HTR-Helium
Brenner, K.G.E.
High Temperature Materials Programme (1981) - c/o Robert Michaels Detection Ltd.

(22) Ternary Diagrams for the Characterization of Metallic Corrosion in High Temperature Reactors
Brenner, K.G.E.
Proc. Conf. on Gas-Cooled Reactors Today,1982, Bristol, UK.

(23) Evaluation of materials for HTR components
Theymenn W. and Jauer H.
Nuclear Energy, 17, vol.4 (1978) p. 321-333.

(24) Chemical Behaviour and Mechanical Performance in HTR-Helium at High Temperatures
Cook R.H. and Graham L.W.
Proc. International Conference on Alloy 800, 1978, Petten

(25) Current status of materials for HTGR at General Atomic company
Roberts D.I.
Proceeding of IAEA specialists Meeting on the high temperature metallic materials for application on gas cooled reactors, 1981, Vienne, Austria

(26) Development and Testing of Alloys for Circuit Structures of a VHTR
Kondo, T.
Proc. IAEA Specialist's Meeting High Temperature Materials for Application on Gas-Cooled Reactors, 1981, Vienna

(27) Iron-base, Oxide Dispersion Strengthened Alloys : basic properties and potential for high temperatures applications
Schuster H.
Proc. of first international spring school & symposium on advances in materials science (SAMS 94), KFA Juelich, 15-20 March 1994, pp 279-300

(28) Impurity measurement test of HTTR (at the commissioning tests)
Sakaba N., Emori K. and Saruta T.
JAERI-Tech 99-072, September 1999

(29) Corrosion behaviour of high temperature alloys in the cooling gas of high temperature reactors
Quadakkers W.J., Schuster H.
High temperature metallic materials for gas-cooled reactors. Proceedings of a specialists meeting held in Cracow, 20-23 June 1988 ; IAEA IWGGCR-18, pp 69-74

(30) Qualification of Metallic Materials for Application in Advanced High Temperature Gas Cooled Reactors
Nickel H., Schubert F., Schuster H., Ennis J.P.
Nuc. Tech. Vol. 58 pp 90-106

(31) Characterization of the Metal-Environment Interactions in Corrosion and Creep of Structural Alloys in the HTR Helium Environments
Kondo T, Shindo M., Kiuchi K.
Proc. of Japan-US Seminar HTGR Safety Technology, 1977, New York, USA, vol. 2, pp 181-194

(32) Environmental conditions in HTRs and the selection and development of primary circuit materials
Graham L.W., Everett M.R., Lupton D., Ridealgh F., Sturge D.W.
Proc. of IAEA Symposium "Gas-Cooled Reactors with Emphasis on Advanced Systems", Juelich, 1976, pp. 319-351

(33) The effect of controlled impurity helium on the mechanical behaviour of hastelloy X
Li C.C., Thomson L.D.,
Nuclear technology, 66 (1984) p. 439-464

(34) Materials for Advanced High Temperature Reactors
Graham L.W.
Rev. Intl. Htes. Temp..et Refract. (1976) p. t-13

(35) Current status of studies in high temperature metallic materials fot HTGR applications in JAERI
Tsuji H., Nakajima H., Kondo T.
Proc. specialists'meeting on high-temperature metallic materials for gas-cooled reactors, pp 81-90, 20-23 June 1988, Cracow, Poland

(36) Mechanical Properties of Heat-Resistant Alloys Exposed to Air and HTGR Helium at High Temperature
Fujioka J., Fukasako N., Murase H
Nucl. Technol. Vol. 66-1 (1984) p. 175

(37) Corrosion of High Temperature Alloys in the Primary Circuit Helium of High Temperature Gas Cooled Reactors - Part II: Experimental Results
Quadakkers W.J.
Werkstoffe und Korrosion, 36 (1985) p. 335

(38) Post service examination of a 10 mW Helium-Helium heat exchanger and comparison with long term behaviour in laboratory tests, Proc. specialists'meeting on high-temperature metallic materials for gas-cooled reactors, pp 129-135, 20-23 June 1988, Cracow, Poland

1. Introduction

This document contributes to the deliverable D45 of the HTR-E project WP6 (helium purification system) of the 5th European FP. It aims at recommending, for metallic materials, the safe range of primary helium environment (impurities content) for a modern direct-cycle HTR (1).

The normal sources of contaminants that are expected in HTR helium coolant are those which are desorbed from reactor components, refuelling operations (residual air, water), air in-leakage, fission products that migrate from the fuel, moisture and contaminants from new helium supply. From former HTRs (with steam generator, i.e. additional water in-leakage risk), the helium impurities (H_2O, H_2, CO_2, CO, CH_4) are expected to be in the 1-100 µbar range.

No deleterious high temperature gas corrosion effect were found in the past on metallic material up to 750 °C (3). However at higher temperatures, impurities content with excessively high or very low carbon activities may cause carburisation or decarburisation, respectively (see Figure 1). In any case it is important to notice that relatively small drifts from the specified impurity content range can produce significant deleterious effects in metallic material during operation at very high temperature.

Unfortunately there is a lack of corrosion data in helium environments at high temperature for current candidate metallic material. Taking into account results of the WP6 2002 work, a parametric approach based on theoretical phase stability diagrams is used in this work. Expected behaviour of chromia former nickel base alloys in helium environment are analysed by locating former and current HTR environments on these diagrams.

Recommendations for helium atmosphere at high temperature with regard to the material aspects are then proposed.

Erosion effects should also have been taken into account due to graphite particles content (dust) which is claimed to be significant in the direct cycle concept. However no relevant data were found on the topic in the open literature.

2. 2002 work results

A review of the literature focused on the basic mechanisms of the interaction between impure helium and metallic materials in HTR reactors has been performed in 2002 (2). The reactivity of the helium environments and the basic reactions involved in the interaction between Ni-base alloys and impure helium are presented as well as their consequences on the behaviour of Ni-base alloys.

Corrosion in helium environment is caused by the reaction of the metal with helium impurities (H_2O, CO, CH_4, H_2, CO_2). Influent parameters are the temperature, the impurity concentration partial pressures (in µatm) and the alloy composition (chromium activity).

The main corrosion phenomena observed and their consequences are:

- Oxidation: loss of thickness (superficial) or ductility loss and cracks formation (internal)
- Carburization: non protection against oxidation (external layers) or ductility loss and cracks formation (internal)
- Decarburization: strength loss.

All these interactions between helium impurities and alloys can be described by the stability diagrams which link the material properties and the environmental conditions, considering that for Ni-base alloys with high Cr and low Al, Cr is the main element governing the corrosion phenomena (see appendix A1).

For a given temperature, good behaviour of high Cr Ni-based alloys is associated with the formation of a chromium oxide layer and low carburization of the alloy. Higher chromium activity increases the stability domains of oxide and carbide, but other oxidizable elements are considered to act by modifying the chromium activity and thus eventually the stability diagrams of the alloy.

This implies for the helium composition:

- P_{CO} > Critical value P_{CO}* = f(chromium activity in material)
- P_{H2O}/P_{H2} > Critical value = f(chromium activity in material)
- P_{CH4}/P_{H2O} < Critical value = f(chromium activity in material)

The above critical values are based on thermo dynamical considerations for the partial pressure of CO and the ratio P_{H2O}/P_{H2} and, in this respect, are easily attainable. The critical ratio P_{CH4}/P_{H2O} is based on relative kinetics of two reactions and will be very dependant on the surface conditions and, in this respect, quite difficult to define precisely.

3. Metallic materials and corrosion effects in HTR helium atmospheres

3.1 Preamble

The behaviour of a material in a given HTR environment is thus mainly a function of chromium activity, and temperature. Stability diagrams are useful tools to predict it, but their use is limited due to the unknown actual chromium activity of candidate materials (depending on the environmental influence of other alloying elements and the possible long term evolution due to chromium depletion of Cr and other oxidizable alloying elements near the surface).

A possible way to locate candidate materials on the diagrams is to correlate their corrosion response for a given set of test conditions (atmosphere composition, pressure, temperature) with the damaging features of one of the seven phase stability domains of the diagram (see appendix A1).

Although such an approach could be a good mean to define limits of use of a particular alloy, it requires numerous helium corrosion tests. In fact, except for some well-known material (namely alloy 800H, alloy 617, Hastelloy X/XR), no data have been found in the open literature for other candidate material (see below).

3.2 Candidate materials

Several metallic materials have been selected in the frame of current studies as candidate material for direct-cycle HTR applications.

- Alloys for circuits and heat exchangers
    - Alloy 800H
    - Alloy 617
    - Hastelloy X and XR
    - ODS (Oxide Dispersion Strengthened) super alloys
- Steels for pressure vessel
    - 9% Cr, 16MND5
- Alloys for turbine blade
    - 2 DS (Directionally Solidified) grades : CM 247 LC DS et IN 792 LC DS (HTR M/M1 selection)

The first three one have been extensively studied for years in the frame of former HTR projects and numerous data are available, in the temperature range 700-950°C (30).

- Alloy 800H is a well-characterized readily available Fe-Ni-Cr alloy that could be used in advanced HTR application requiring intermediate temperature capability.

- Alloy 617 has been the reference material for high temperature components in the last German HTGR projects. It is one of the strongest wrought solid solution hardened nickel-base alloys, which can be hot and cold worked to plate, sheet, and tube.

- Hastelloy X is a nickel-based solid solution strengthened alloy, with creep-rupture strengths that lie between those of Alloy 617 and Alloy 800H. Hastelloy XR is an optimized version of Hastelloy X with low Co and Al content and improved control of the concentration of low alloying and residual elements (Mn, Si, …).

ODS (Oxide Dispersion Strengthened) superalloys and DS (Directionally Solidified) grades alloys are output data from the HTR-M. ODS alloys have been developed for high temperature components in aggressive environments. They exhibit excellent corrosion resistance as well as high creep strength at temperature up to 1100°C. Unfortunately they have never been tested in HTR helium atmosphere, all studies being devoted to air oxidation.

The 9% Cr (X10CrMoVNb 9.1) and possibly 16MND5 steels are foreseeing to be used as primary vessel material but no experimental data are available in HTR helium atmospheres.

- 9% Cr is a martensitic steel material for use at temperature up to about 500°C ;

- 16MND5 is low alloyed steel used for the PWR primary vessel (T<375°C).

These materials can be oxidized at low temperature but also they can suffer some carburization or decarburization which can become significant above ~ 500 ° C.

DS grades are output data from the HTR-M: CM 247 LC DS is an Al-oxide former and IN 792 LC DS is a Cr-oxide former. No corrosion data found in helium atmosphere for these alloys.

3.3 Review of main helium compositions

The general knowledge concerning the HTR helium atmosphere and the related corrosion behaviour of material arises either from the feedback of operated reactors or from the numerous lab- and test-loop experiments performed throughout the world, especially in Germany.

The Table 1 displays various material-related helium-simulating environments found in the literature. Note that PNP helium[1] is a standardized test gas defined in Germany to carry out investigations concerning the corrosion behaviour of alloys with the same simulated HTR helium in different laboratories.

The helium environment is expected to be a low-oxygen-potential environment with enhanced carburization kinetics. In the impure helium atmospheres, oxygen activity is set by H_2O and H_2 content, carbon activity is set by CO content (thermodynamically) and by CH_4 content (kinetically)[2]. The oxygen partial pressure P_{O2} and the carbon activity a_C are input data for the building of phase stability diagrams described in appendix A1.

---

[1] PNP means "Prototype Plant for Nuclear Process Heat", a German HTGR project aiming at the use of nuclear heat for the steam gasification of hard coal and steam reforming of methane coupled to the hydro gasification of lignite.

[2] Effect of CH_4 level :

The helium coolant in a direct-cycle gas-turbine is expected to be much drier (i.e. high ratios H_2/H_2O) than in the case of a steam-cycle system where continuous ingress of low levels of water and steam is possible (i.e. low ratios H_2/H_2O). On the other hand, less H_2 content resulting from steam circuit corrosion can also be expected, which would in fact lead to maintain similar H_2/H_2O ratios in the primary circuit.

Concerning dusts, it is claimed that higher dust content in the primary circuit are anticipated due to higher flow rate variations in a direct-cycle HTR.

In addition, specificities of helium purification system for a current direct-cycle type reactor (GT-MHR) are given in appendix A2.

- At low CH_4 content, carburizing and oxidizing values are linked by the following equilibrium existing in surface pores (consequence of the microclimate reaction – see § 3.4.4).

$$CO + H_2 \rightarrow C + H_2O$$

- At high CH_4 content (typically $P_{CH4} > 100\ P_{H2O}$ content), $a_C = 1$. The oxidizing value only depends on the CO content.

3.4 Bibliographical analysis: corrosion phenomena in HTR helium environments and their consequences

The reactions of the gaseous impurities, H_2, H_2O, CO and CH_4 which are present in the primary cooling helium at the surface of high temperature alloys (fabricated mainly from Ni(Fe)Cr) lead to corrosion effects which can significantly influence the mechanical properties of the alloys (4).

The main corrosion phenomena observed are oxidation, carburization and decarburization (5), (6), (7). The formation of a protective stable oxide layer results of the presence of water in sufficient proportion (P_{H2O}/P_{H2}> critical value) and of the balance between oxidation and carburization reactions which are a function of both thermodynamics and kinetics factors. Because of the rapid flow rate in the core and because of the low partial pressure of reactive impurities, the gas can not reach its equilibrium state. The corrosion behaviour will be determined by the kinetics of the individual gas metal reactions.

Carburization and decarburization can adversely affect long term properties such as creep and fatigue and short term properties such as fracture toughness (4). It has however been demonstrated that for certain alloys there are gas environments where the degree of carburization/decarburization is small and acceptable (8).

For describing the corrosion behaviour of a Ni(Fe)Cr based high temperature alloys, chromium is initially considered as the only oxide and carbide forming element. The phase stability diagrams developed by Quadakkers (5), (20) and depicted in appendix A1 are used to predict this corrosion behaviour. These representations are based on the stability diagram of chromium oxide and chromium carbides as a function of the impurity content of helium expressed as the carbon and oxygen activities, a_C and P_{O2}.

Note that another approach given by Brenner (12), (21), (22) can be used. This approach isn't described here.

The influence of minor additions of strong oxide formers (e.g. Al, Ti, Mn) is in most cases restricted to the initial periods of the corrosion process. Due to the small amounts of these elements usually present in the alloy, their concentration at the interface between surface layers (oxide, carbide) and the alloy decreases to practically zero after long exposure times.

We are now going to describe each of the main corrosion process with the related chemical reaction and the consequences on the mechanical properties of materials.

3.4.1 Carburization

Carburization occurs when the carbon potential in the material is lower than in the gas. A carbon transfer is so possible and leads to the formation of carbides. Two kinds of carbides are commonly found: C_6Cr_{23} et C_3Cr_7. The composition and the stoichiometry of the carbides depend of the alloy composition and the carbon solubility.

Two impurities of the helium lead to the formation of carbides: CH_4 and CO.

For example :

$$23\ Cr + 6\ CH_4 \leftrightarrow C_6Cr_{23} + 12\ H_2 \quad (1)$$

CH_4 is not stable at a temperature upper than 800°C, so the consumption of CO is possible:

$$27\ Cr + 6\ CO \leftrightarrow C_6Cr_{23} + 2\ Cr_2O_3 \quad (2)$$

Two forms of carburization are possible:

Formation of a superficial non protective layer of blocky carbides:

This occurs in the domains IV and V of the stability diagram (see figure A1-1 in appendix A1). In zone IV of the diagram, this layer interferes with the oxidation process and can inhibit the formation of a protective oxide layer (see Figure 12). This results in a porous layer which may allow both severe oxidation (domain IV) and carbon access to the bulk material and carbide formation when the solubility limit is reached (see below).

As shown in Figure 3, all of the 3 alloys, alloy 617, alloy 800H and Hastelloy X can develop surface scale consisting of M- and/or Cr-rich oxides and Cr-rich carbides in the domain IVb of the diagram (11).

The carbides formed in such a scale can become unstable due to local increases in oxygen potential (operating conditions) or decreases in chromium activity (depletion – see above). Additional carbon atoms generated by surface carbide dissociation become available to carburise the metal underneath the scale, leading to enhanced carburization effects.

In-depth carburization of the alloy by carbon diffusion into the matrix:

This occurs in the domains III, IV and V of the stability diagram. In the domains IV and V, this internal carburization may be fast because there is no protective layer. In the domain III, it is limited by the presence of a compact oxide layer. The kinetics of carburization, associated with a mass gain, is often parabolic and increases with temperature. Carbide formation may be intra- or inter-granular.

The formation of carbides is shown in Figure 4 which describes the uptake of carbon for three kinds of alloys as a function of the temperature. This increase is linear or exponential depending on the alloy and on the presence and efficiency of the protective oxide layer (7).

As an example, fast carburization of alloys like alloy 800 can occur under strongly reducing conditions (i.e. at a very low oxygen activity). If no protective oxide layer is present, the rate of the carburization is determined by the carbon diffusion into the material (2).

Another example of microstructure affected by an intra- and inter-granular carbides formation is given by the Figure 2. The carburized depth of Alloy 617 exposed to a 1000°C helium atmosphere during 5000 hours is of several hundred of microns (19). Increasing the silicon content of the alloys limits the carbon solubility and so the carbides formation, particularly when the ratio Fe/Ni is around 0,2 (8).

The internal carburization causes an embrittlement of the alloy by altering ductility and strength of the material (9), (11). It is illustrated by the Figure 5 which described for alloy 800H and Alloy 617 the effect of the carbon uptake on the tensile strength at ambient temperature (10).

An extreme form of carburization is called metal dusting. In this case (very low oxygen pressure and carbon activity >1), chromium is precipitated as carbides and the iron nickel matrix (alloy 800 for example at 1000°C) is converted to a mixture of metal, graphite and oxide (2).

3.4.2 Decarburization

Decarburization results of the reaction between carbon and water, which can also disturb the oxide formation because of gas bubble formation.

$$H_2O + [C] \leftrightarrow CO + H_2 \quad (3)$$

This reaction (3) lowers the carbon contents of the matrix until it becomes too low and then carbides are unstable and can be dissolved:

$$M_yC_x \leftrightarrow y\ M + x\ C \quad (4)$$

For the chromium carbides, the global reaction is:

$$C_6Cr_{23} + 6\ H_2O \leftrightarrow 23\ Cr + 6\ CO + 6\ H_2 \quad (5)$$

The Figure 6 illustrates the microstructure of alloy 617 after 2500 hours in a 950 °C helium atmosphere.

Some very high temperature alloys take their good mechanical behaviour from solid solution effects and carbide precipitates. These mechanical properties will drop if the decarburization occurs. For example the creep behaviour is correlated to the decarburization as shown on the Figure 9**.** The mechanical properties of alloys oxidised in helium are similar than in air. The oxidation phenomenon is assumed to be protective for the alloys.

Globally, the decarburization phenomena induce a loss of creep resistance associated to the dissolution of the carbides. For the Hastelloy XR in a 950°C helium with a variable composition (He-1 to He-4), the resistance of the decarburised sample (He-3) is lower than with the carburized (He-1 & He-2 - see Figure 10). The creep life time is also dependant on the helium composition, higher in the domain III than in the domain II and IV (see Figure 11).

3.4.3 Oxidation

In HTR environment, most of the oxygen reacts with the graphite of the reflectors. Thus, the partial pressure of oxygen is in the range of 10^{-15} to 10^{-25} atm (15). The oxidation potential of the gas is given by the ratio P_{H2O}/P_{H2}.

This is illustrated by the following reaction:

$$y\ Me + x\ H_2O \leftrightarrow Me_yO_x + x\ H_2 \quad (6)$$

Concerning the chromium it gives:

$$\frac{2}{3}\ Cr + H_2O \leftrightarrow \frac{1}{3}\ Cr_2O_3 + H_2 \quad (7)$$

The formation of an oxide layer is the safest situation for an alloy in HTR gas environment if this one is compact and dense. Such a layer avoids the contact between impurities and the alloy. If it is porous or cracked, internal oxidation and carburization are possible. The formation of chromium oxide is favourable because this oxide is stable in a wide temperature range. Chromium is also the principal element able to form an oxide layer (with Al, Ti, Mn and Si). It can also form carbides which can interfere with the oxide formation (7). This is illustrated by the Figure 13.

Internal oxidation results mainly of the presence of minor elements with a very high negative values of free energy of formation of oxides (mainly Al, Si) (13). Internal oxidation occurs if the diffusion rate of minor elements toward the outside is lower than the oxygen diffusion rate towards the inside. Oxidation then takes place inside the matrix and may be intergranular (see Figure 3 and Figure 14).

Internal oxidation may impair the mechanical properties mainly by favouring the crack initiation on intergranular oxides at high temperature (24).

For some alloys with a high level of aluminium (IN 713 LC for example), the depth of the internal oxidation is around 25 µm, after 5000 hours in a 900°C helium (11).

3.4.4 The microclimate reactions

This particular reaction plays a major role for the corrosion phenomena in HTR environments. It appears that above a given temperature for a given CO partial pressure P_{CO}, the carbon monoxide is more stable than the carbide and the oxide. It can be illustrated by the reaction:

$$2\ Cr_2O_3 + Cr_{23}C_6 \leftrightarrow 6\ CO + 27\ Cr \quad (8)$$

The direct reaction (8) cannot occur because it involves two solid reactants. Nevertheless, in pores, it can result from the following partial reactions occurring in a locally confined gaseous atmosphere.

$$6\ H_2 + 2\ Cr_2O_3 \leftrightarrow 6\ H_2O + 4\ Cr \quad (9)$$

$$Cr_{23}C_6 \leftrightarrow 6\ C + 23\ Cr \quad (10)$$

$$6\ C + 6\ H_2O \leftrightarrow 6\ CO + 6\ H_2 \quad (11)$$

(9)+(10)+(11) lead to (8).

The 3 reactions below also result, for another type of carbide, from the local equilibrium of gaseous phases:

$$\frac{7}{3}\ Cr + C \leftrightarrow \frac{1}{3}\ Cr_7C_3 \quad (12)$$

$$CO \leftrightarrow C + \frac{1}{2}\ O_2 \quad (13)$$

$$\frac{2}{3}\ Cr + \frac{1}{2} O_2 \leftrightarrow \frac{1}{3} Cr_20_3 \quad (14)$$

(12) + (13) + (14) leads to (15)

$$3\ Cr + CO \leftrightarrow \frac{1}{3}\ C_3Cr_7 + \frac{1}{3}\ Cr_2O_3 \quad (15)$$

The microclimate reaction depends of a critical partial pressure of CO (P_{CO}*) or a critical temperature (Ta). If $P_{co} < P_{CO}$* or T<Ta the microclimate reaction does not occur.

The occurrence of the phenomenon described is thus a function of the environment (temperature, gas composition) and the alloys composition (see appendix A1). This is well described by the Figure 20.

Under low partial pressure of CH_4, the shift between carburization and decarburization is a function of the temperature and the water pressure. This is described by the Figure 7 (under condition of microclimate reaction). When increasing the level of water, the carbon content on the alloys decreases, which illustrates the decarburization phenomena.

It is also well described by the Figure 8. The inlet part of a sample is exposed to a flow of helium containing water which is quickly consumed in such a way that the outlet part of the same sample is exposed to helium with no more water. The consequences are clear. The inlet part is decarburised and the outlet part is still carburised.

3.4.5 Oxidation and carburization

Oxidation and carburization can occur simultaneously. The Figure 12 illustrates the morphology of Alloy 617 after exposition in a 900°C helium (12). On the surface the clear and external layer is composed of carbides and the inner dark layer is the oxide. An internal oxidation is also observed below and the formation of inter- and intra-granular carbides.

The carbon monoxide can also play the role of oxidant leading to the formation of a combined layer made of oxide and carbide. These kinds of films are not protective against corrosion.

The following reactions can occur:

$$CO + Me \leftrightarrow MeO + [C] \quad (16)$$

$$6\ CO + 27\ Cr \leftrightarrow 2\ Cr_2O_3 + C_6Cr_{23} \quad (17)$$

This phenomenon is governed by the microclimate reaction described above.

3.4.6 Nitriding

At high temperature, alloy nitriding is a risk to be considered (36). N_2 impurities in the helium atmosphere can diffuse into the bulk material and could lead to modify the mechanical properties of the surface (hardening).

3.4.7 Evaporation and spallation

For the higher temperatures (T > 950°C), a possible evaporation of the external layer can be observed. This is the case for example for the Hastelloy X and XR (16) (see Figure 15). The evaporation leads to the formation of whiskers on the surface such as illustrated by the Figure 16.

The spallation is also observed in the case of thermal cycling (see Figure 17) (17) or when the layers are thick and subjected to external stresses.

3.4.8 Chromium depletion

Even in the "passive" regime (domain III of the stability diagram), a surface chromium depletion is observed with the development of the chromium oxide layer, resulting in a lower content of chromium at the interface metal/oxide. This is illustrated by the Figure 18 (5). The alloy composition evolves with the time and can be in this case more susceptible to corrosion phenomena.

4. Consequences for the helium impurity specifications and management

4.1 Chromia former (high Cr) Ni-base alloys

The stability diagrams are very useful to describe the behaviour of a material considering the composition (impurities levels) of the HTR-Helium. We can estimate, for a given temperature and a material defined by its chromium activity a_{Cr}, whether this composition corresponds or leads to the formation of a protective oxide layer (domain III of the diagram).

We have build stability diagrams for the temperature of 950 °C and 1000°C from theoretical thermodynamics value by considering several chromium activities, a_{Cr}, and we have looked at the position of a few HTR-Helium compositions in this diagram (see the composition of former HTR-Helium in Table 1).

At a temperature of 950°C (see Figure 21), for an alloy with a_{Cr} = 0,6, most of the HTR-Helium compositions are in the domain III, except for the DRAGON-Helium. But if we consider that the oxidation causes a surface chromium depletion leading to a_{Cr} = 0,3, the PNP composition is no more in the safety range, because its nominal CO partial pressure is lower than the critical value P^*_{CO}.

The Figure 19 illustrates this point: the evolution with time of the main corrosion phenomena (oxidation, decarburization, internal oxidation) in a 950°C PNP helium atmosphere is consistent with the occurrence of the microclimate reaction that destabilizes the oxide layer, promotes decarburization and allows intergranular oxidation, with parabolic kinetics.

At a temperature of 1000°C, higher chromium content is needed to be in the safety area. We can notice (see Figure 22) that the KVK and the AVR composition are still in the good range of composition to prevent the microclimate reaction and an excessive carburization for a chromium activity of 0,6. But the microclimate reaction is likely to occur after surface chromium depletion.

These results mean that to establish the best helium composition for the future reactors, it is necessary to consider the temperature and the material evolution in order to guarantee the safest behaviour for long duration. It is worth noticing that helium composition guarantying a safest behaviour at high temperature should insure larger safety margins at any lower temperature.

As an example, assuming that Cr depletion will reduce to 0,3 the surface Cr activity of a Ni-base alloy, safe behaviour will require the following environments:

<u>At 950° C:</u>

- P_{O2} in excess of a critical value of about 2.10^{-23}, i.e. P_{H2O}/P_{H2} ratio in excess of a critical value of about a few 10^{-4} in order to allow the formation of a protective Cr based oxide layer ;
- P_{CO} in excess of a critical value of about 150 µbar to avoid the "microclimate reaction" ;
- P_{CH4}/P_{H2O} lower than about 10^{-2} in order to avoid carburisation and reduction of oxide layers by the methane.

At 1000° C:

- P_{O2} in excess of a critical value of about 10^{-21}, i.e. P_{H2O}/P_{H2} ratio in excess of a critical value of about a few 10^{-4} ;
- P_{CO} in excess of a critical value of about 500 µbar.
- The critical value of the ratio P_{CH4}/P_{H2O} at 1000° C is not available since it results from the relative kinetic of two reactions and no data are available from the literature at this temperature.

4.2 Alumina former (Low Cr – high Ti/Al) Ni-base alloys

Safe behaviour of low Cr – high Ti/Al alloys requires that the formation of a continuous protective alumina layer is not impaired by the oxidation of Cr. Thus the environment must not be too oxidizing, i.e. P_{H2O}/P_{H2} < critical value increasing with temperature.

This critical value should be close to the thermodynamic limit for Cr oxidation and thus basically incompatible with the safe behaviour of chromia former alloys.

Consequently, simultaneous use of both types of Ni-base materials should probably require:

- use of high Cr alloys at lower temperature (higher stability of Cr oxides)
- use of low Cr-High Al/Ti Alloys at high temperature
- severe control of water partial pressure within a quite narrow range.

Thus, this situation should be avoided as long as possible.

4.3 Management of helium impurities in modern HTRs

It is important to notice that the helium specifications for chromia former Ni-base alloys would be defined by considering that most of the impurity pressures or pressure ratios must be higher than a critical value and **this is not consistent with the current specifications** for future reactors which involve:

- impurity level expressed in vpm, which results in actual partial pressure depending on the total helium pressure (and possible pressure variation) in the reactor ;
- highest values of CO or (CO+ CO_2). For the GT-MHR specification (see annexe 2), this maximum is of the order of 6 vpm which results in a maximum partial pressure of CO of 420 µatm under 70 bars of total pressure. This does not insure that the microclimate reaction will be always impossible. Another recommendation anticipates a CO content lower than 2 vpm which would lead to partial pressure lower than 140 µbar (70 bars of total pressure). This would almost necessarily allow the microclimate reaction to occur at temperatures of 950° C.
- highest values for H_2 and H_2O that does not give any indication on the effective P_{O2} of the helium.

Since the kinetic of material degradation is thermally activated, damaging interactions between helium impurity and Ni base alloy would be too large to be tolerated above 850/900° C as it was possible at lower temperature.

Accordingly, the management of helium impurities in modern HTRs working above about 900 °C cannot rely on the simple concept of helium purification which tends to decrease as far as possible all impurity content without discrimination, but **should evolve towards a helium impurity control**. The target values of controlled impurity levels have to take into account the theoretical critical values presented above with additional safety margin to be evaluated from the variation of the operating parameters and the long term evolution of surface composition.

For example, the effect of significant pressure variations in a direct cycle plant may require some margin on the target value of the CO content.

Of course, all the above requirements on helium impurity control are only related to Ni-base alloys. The final specifications have also to deal with the interaction of helium impurities with the graphite. This may lead to upper values of P_{H2O}/P_{H2}, but the presence of significant partial pressure of CO should not be deleterious to the graphite.

5. Conclusion

The work performed in 2002 has summarized the main reactions that can occur on the surface of a Ni-base alloy exposed to HTR helium at high temperature and the main effect of gas impurities and Cr activity of the alloy on these reactions. The use of phase stability diagrams to evaluate the surface reactions and the different domains of predominance of the surface reactions has been presented. This shows that a safe behaviour of chromia forming Ni-base alloys in HTR helium requires at least three conditions:

- P_{H2O}/P_{H2} > critical value to allow the formation of a protective oxide layer
- P_{CO} > critical value to avoid the microclimate reaction
- P_{CH4}/P_{H2O} < critical value to avoid the carburization and oxide reduction by the methane

All these critical values are dependent on the temperature and Cr activity. Higher the temperature, higher the critical values of P_{H2O}/P_{H2} and P_{CO}.

However, the determination of the phase stability diagrams requires the knowledge of the Cr activity of the metallic alloy which is dependent both on the other alloying elements and on the metallurgical condition of the material. In addition, the surface reaction may cause a surface depletion of oxidizable elements which can modify the critical values of P_{O2} and P_{CO} required for a safe behaviour of the high Cr Ni base alloys.

This report summarizes the behaviour of materials observed as a function of the HTR compositions and determined the location of the main compositions of past HTR helium in stability diagrams drawn for very high temperature. This shows that helium compositions such as PNP that are safe at relatively low temperatures (typically < 850 °C/900 °C) may not be safe at higher temperatures.

Assuming values of surface Cr activities of about 0,3 under a protective oxide layer, order of magnitudes of the critical values to be specified for a safe behaviour of Ni-base alloy can be derived as follows:

- **at 950° C, $P_{O2} > 2.\ 10^{-23}$, i.e. P_{H2O}/P_{H2} > a few 10^{-4} and P_{CO} > ~ 150 µbar**
- **at 1000° C, $P_{O2} > 10^{-21}$, i.e.P_{H2O}/P_{H2} > a few 10^{-4} and P_{CO} > ~500 µbar**

In addition, higher the temperature, faster the kinetics of material degradation. Thus, higher the temperature, more strict must be the enforcement of the above helium specifications. Thus, for modern HTRs working at very high temperatures (typically above 850/900° C), the management of the impurities of the helium cannot be based on a simple purification process which tends to remove all impurities form the environments without discrimination. Some form of impurity control is rather required.

This review also shows that the precise determination of the helium specification requires more work particularly in the following areas:

- modelling the Cr activity of the alloys and its evolution on the alloy surfaces with time in the HTR environment,

- constraints related to the oxidation of graphite at high temperature and the possible formation of C dust and CO_2 in the low temperature regions,

- evaluation of the need for N_2 specification.

Regarding the characterization of the behaviour of Ni-base alloys in HTRs there is also significant lacks of knowledge:

- Consistent set of experimental data are available only for a few material, mainly alloy 800 at moderate temperature and alloy 617 (and to some extent Hastelloy X) up to 950/1000 °C, but possible new materials will need a complete characterization.
- Complementary studies are still required on the above materials particularly to establish their maximum temperature of use. This includes :
  - surface film evaporation at high temperature,
  - possible break away leading to oxide spallation on the HT materials.
- Possible deleterious nitriding effects at high temperature should be evaluated.
- Finally, the possible degradation by erosion by dust present in the environment should be considered.

Figure 1

High temperature gas corrosion effects (T > 750 °C) on metallic materials: Comparison of scale depths and internal oxidation as well as carbon free zone and carbon pick up in exposed IHX tube (HTMP program)

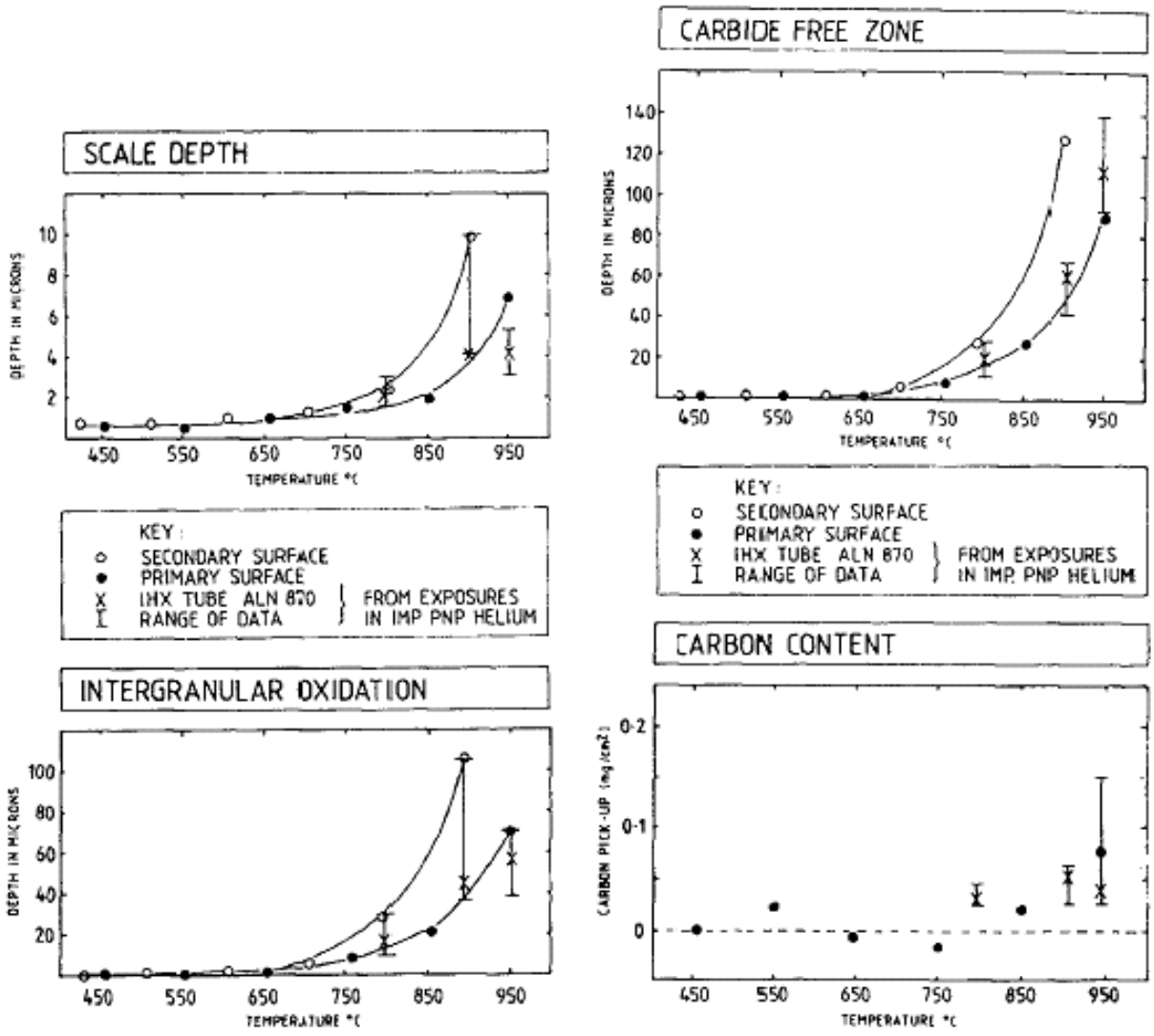

Figure 2

Intra- and inter-granular carbides formation in Alloy 617 exposed during 5000 hours in a 1000 °C helium (H_2O: 0,1 µbar; H_2: 500 µbar ; CO: 1,5 µbar ; CH_4: 2 µbar) (from (19))

Figure 3

Oxide-carbide duplex scale formed on metal surfaces exposed for 3000 h in a 950°C helium (H_2O < 0,5 µbar; H_2: 500 µbar ; CO: 50 µbar ; CH_4: 50 µbar) (from (11))

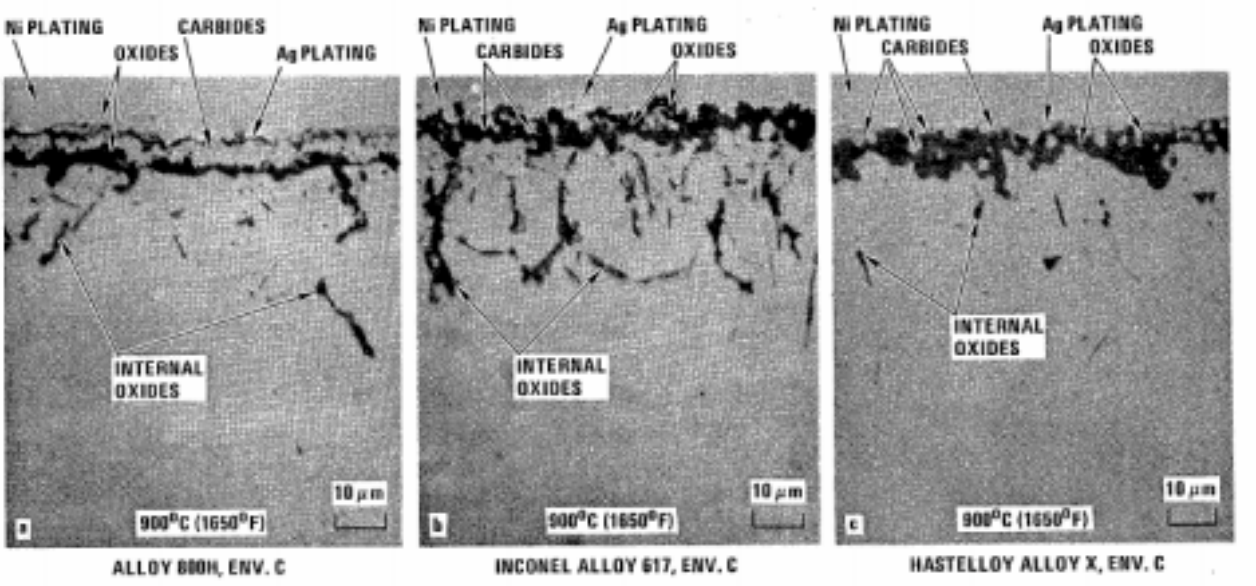

Figure 4

Evolution of the carbon content for three kinds of alloys as a function of the temperature (from (8))

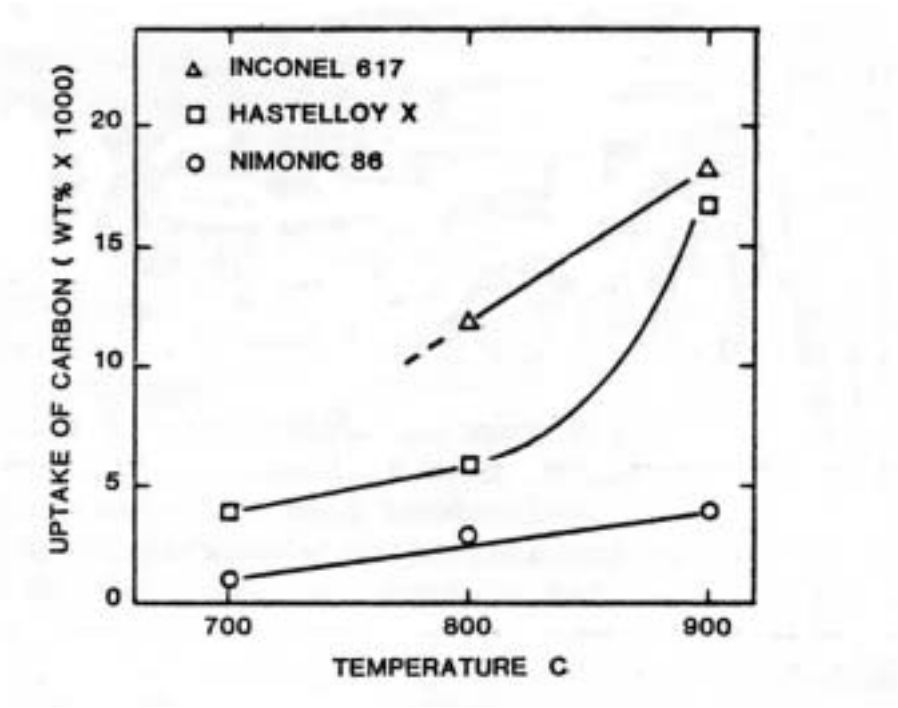

Figure 5

Tensile tests with carburised Alloy 800H and Alloy 617 samples: evolution at ambient temperature of the elastic limit and the rupture elongation with the carbon content (from (10))

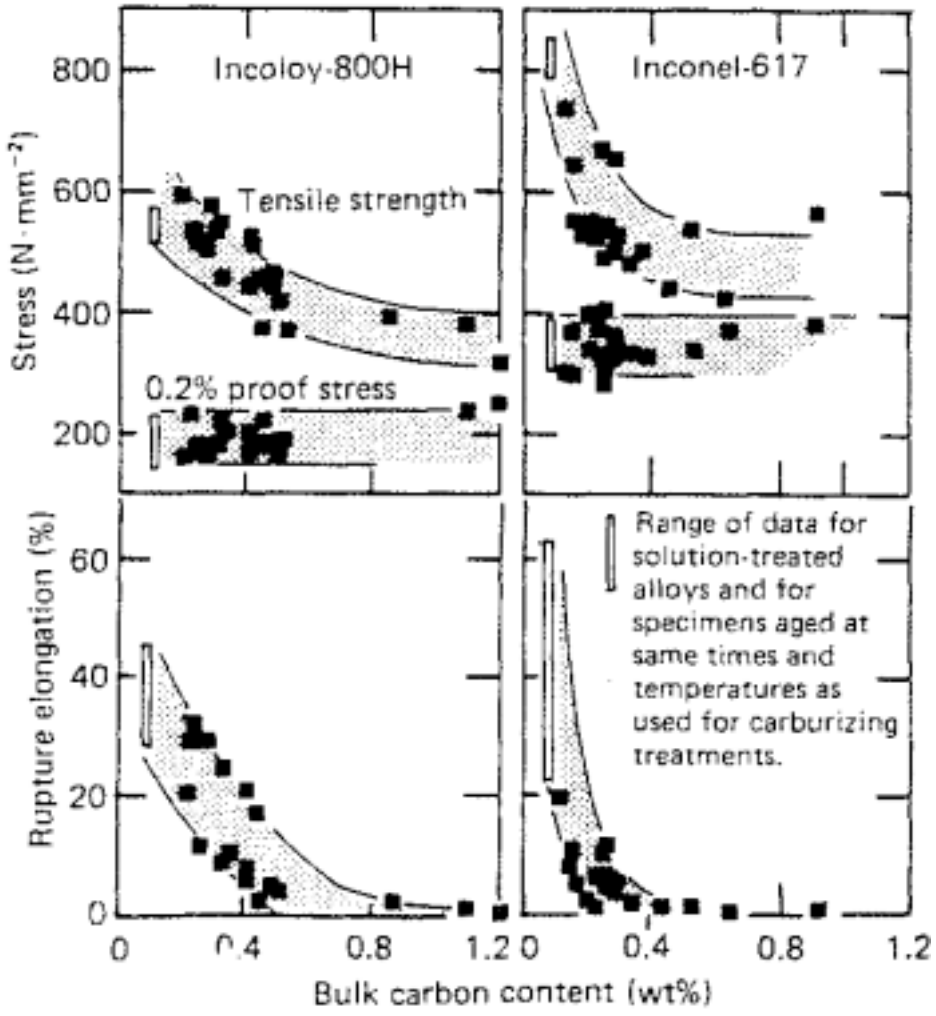

Figure 6

Microstructure of the Alloy 617 after 2500 hours in a 950 °C helium atmosphere (H_2O: 1 µbar ; H_2: 500 µbar ; CO: 5 µbar ; CH_4: 5 µbar) (from (19))

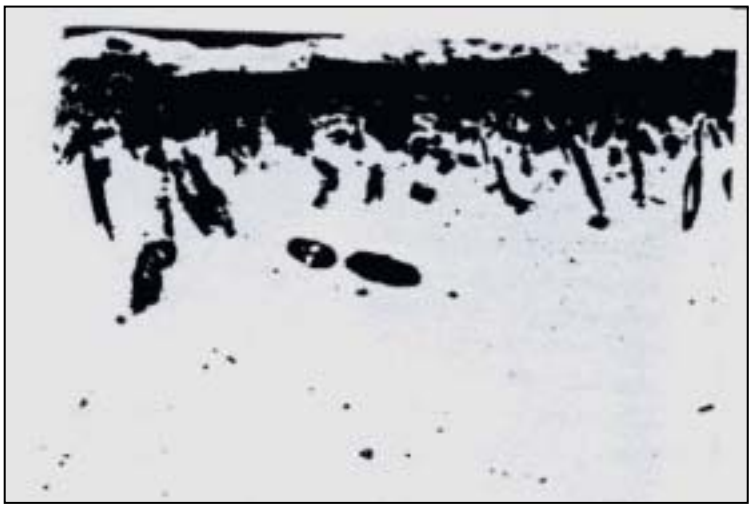

Figure 7

Effect of the water content in a 900°C PNP helium atmosphere on the carburization/decarburization of Hastelloy X for 3000-hour duration (from (7))

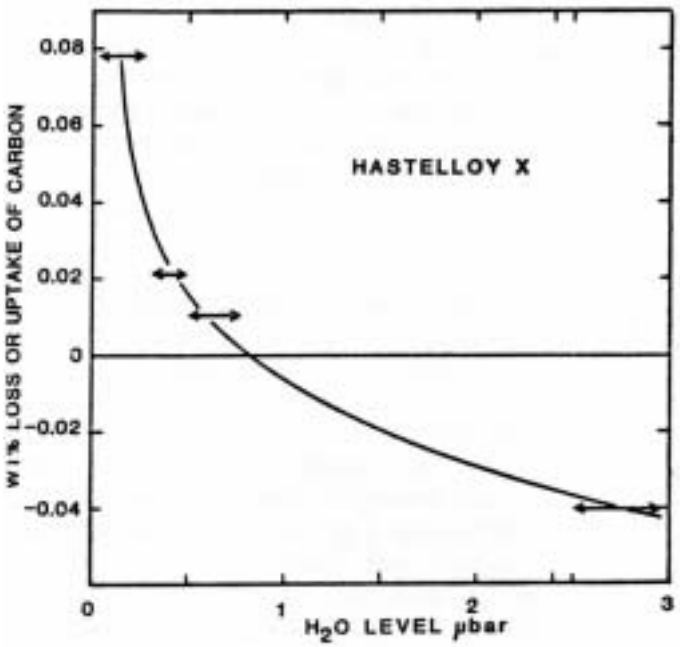

Figure 8

Effect of the water depletion in a flow of helium on the surface reaction for Hastelloy in a 1000°C Helium during 3000 hours.
Due to the consumption of water, the type of damages change from the inlet to the outlet parts (from (7)).

INLET SPECIMEN: decarburised −0.028 %C

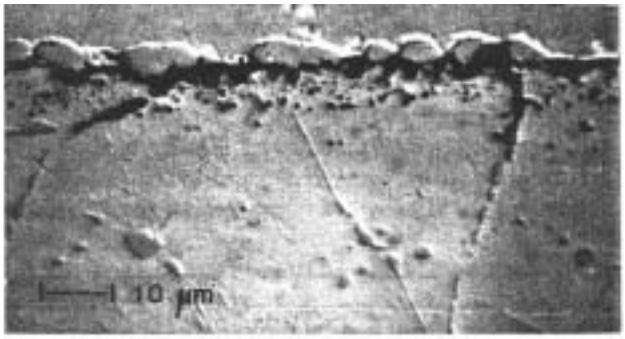

OUTLET SPECIMEN: carburised +0.016 %C

Figure 9

Creep curves of alloy 800H at 800°C in different atmospheres (from(33))

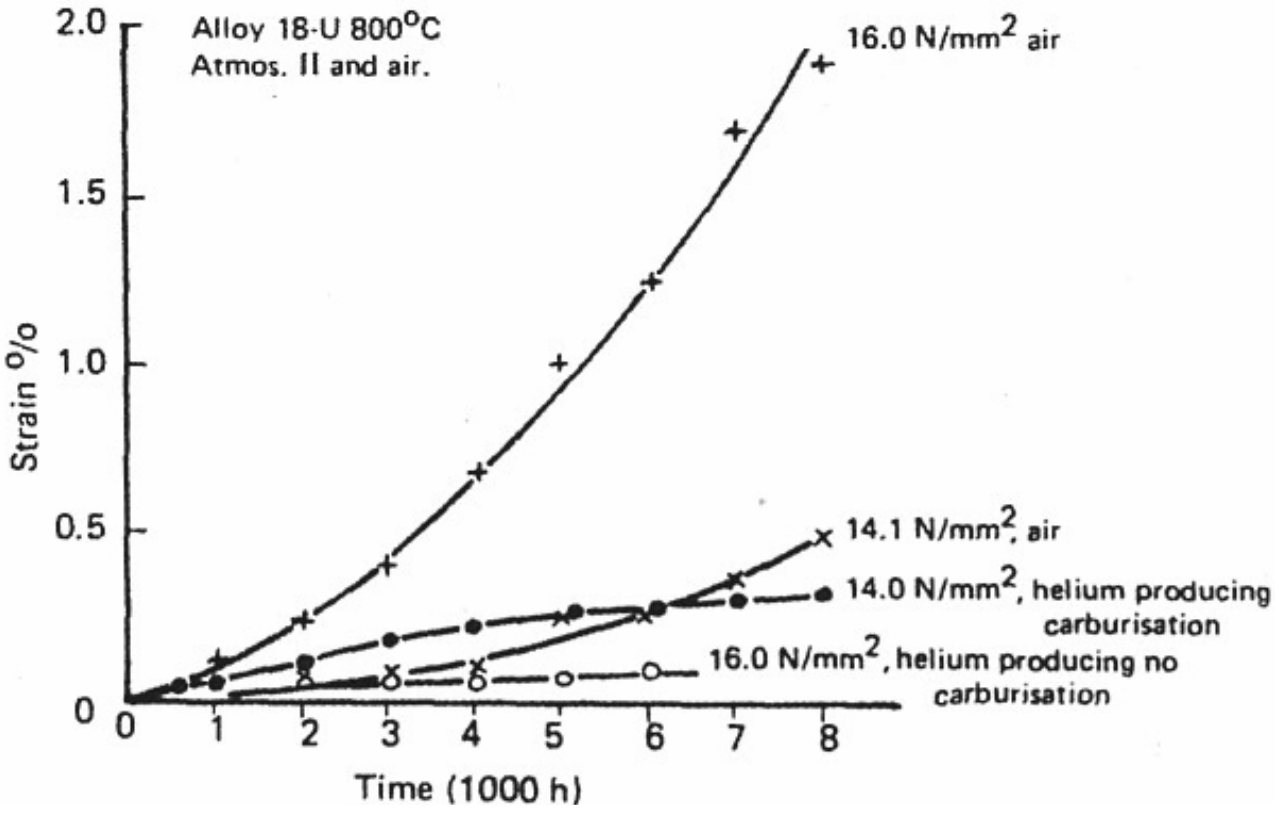

Figure 10

Creep test for Hastelloy XR at 950°C in different Helium compositions (from (34))

He-1: H_2: 200 µbar, H_2O: 1µbar, CO: 100µbar, CH_4: 5 µbar, CO_2: 2 µbar ;
He-2: H_2: 50 µbar, H_2O: 1 µbar, CO: 25 µbar, CH_4: 5 µbar, CO_2: 2 µbar;
He-3: H_2: 500 µbar, H_2O: 1µbar, CO: 3 µbar, CH_4: 5 µbar ;
He-4: H_2: 500 µbar, H_2O: 0,05 µbar, CO: 3 µbar, CH_4: 5 µbar

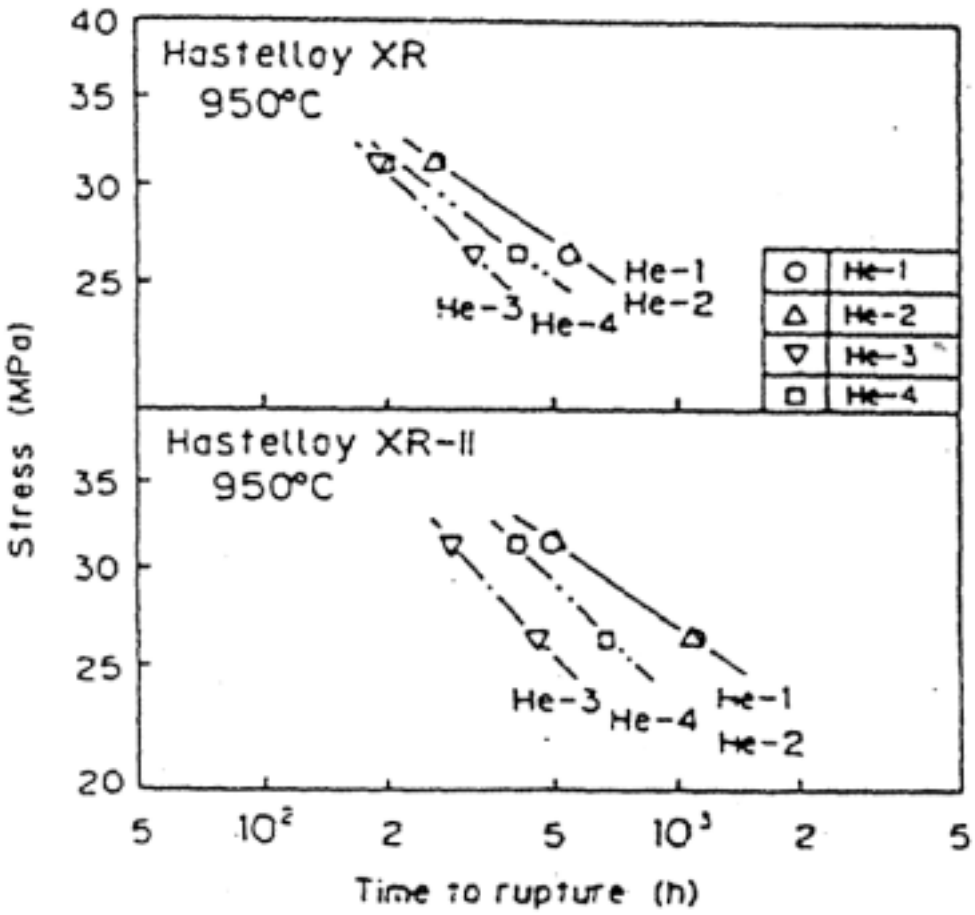

Figure 11

Creep life time for Hastelloy XR at 950°C in different Helium compositions (from (34))

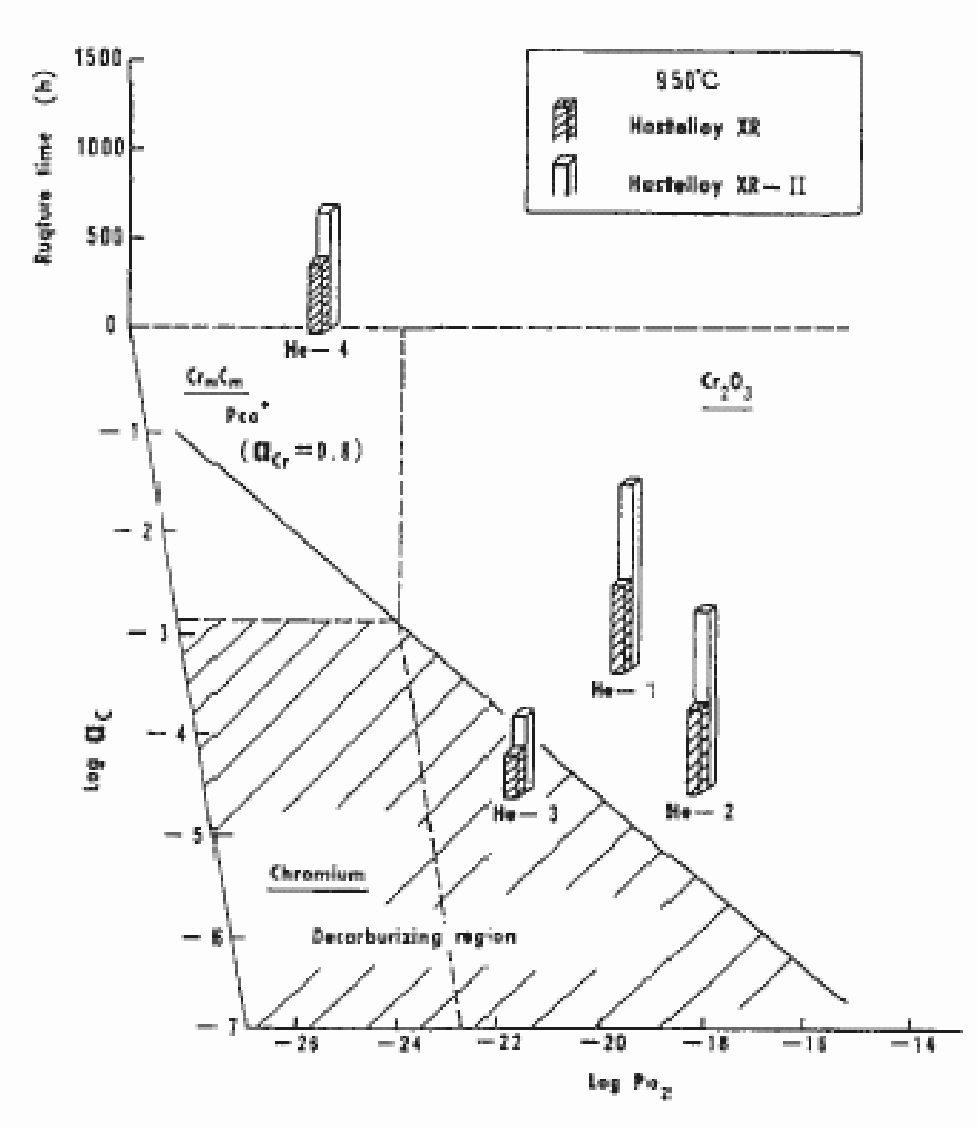

Figure 12

Microstructure of Alloy 617 after exposition in a 900 °C helium atmosphere (H_2O: 0,3 µbar ; H_2: 500 µbar ; CO: 40 µbar ; CH_4: 5 µbar) : oxidation and carburization (from (12))

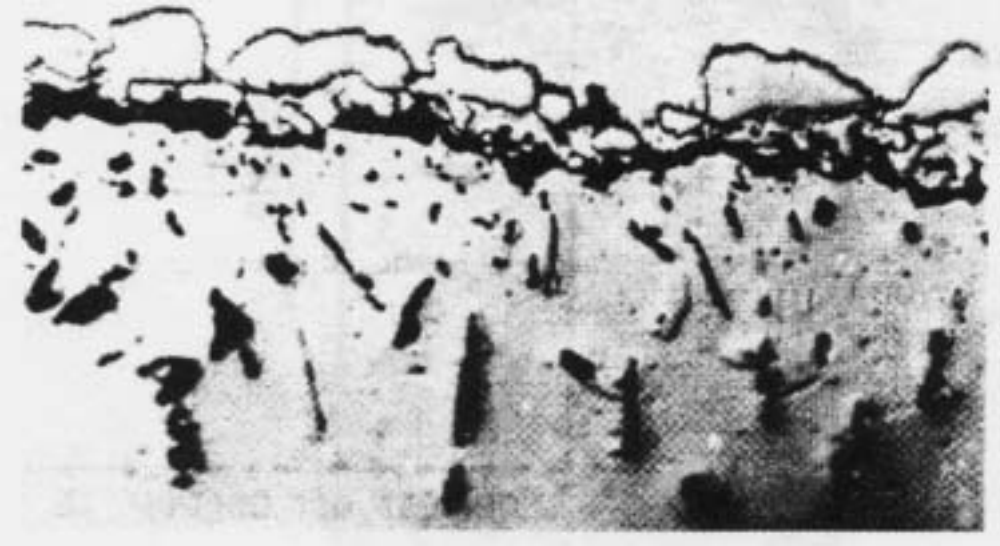

Figure 13

Development of a protective oxide scale on NIMONIC 86 exposed at 900°C in PNP standard test atmosphere (from (7))

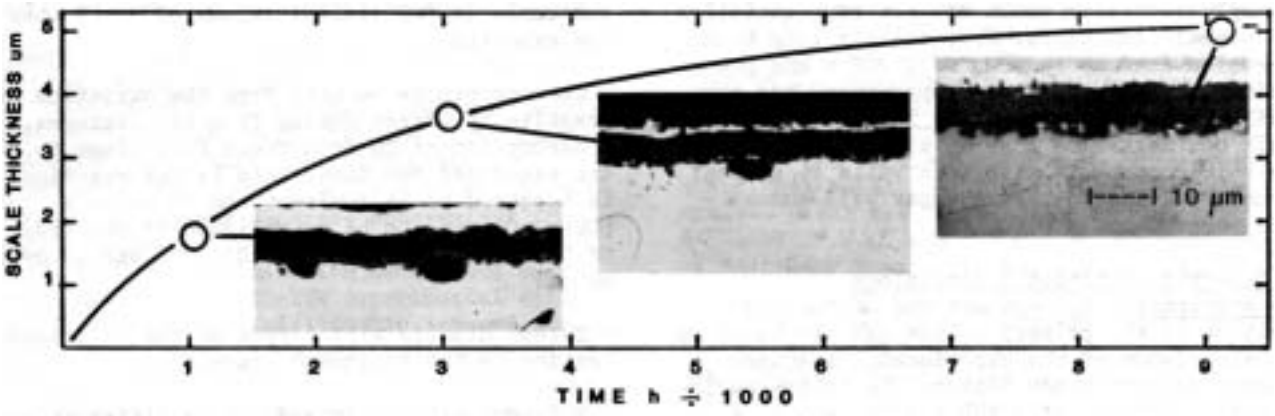

Figure 14

The development of an oxide scale and internal oxidation on two heats of Alloy 617 in a 900°C PNP helium atmosphere (from (14))

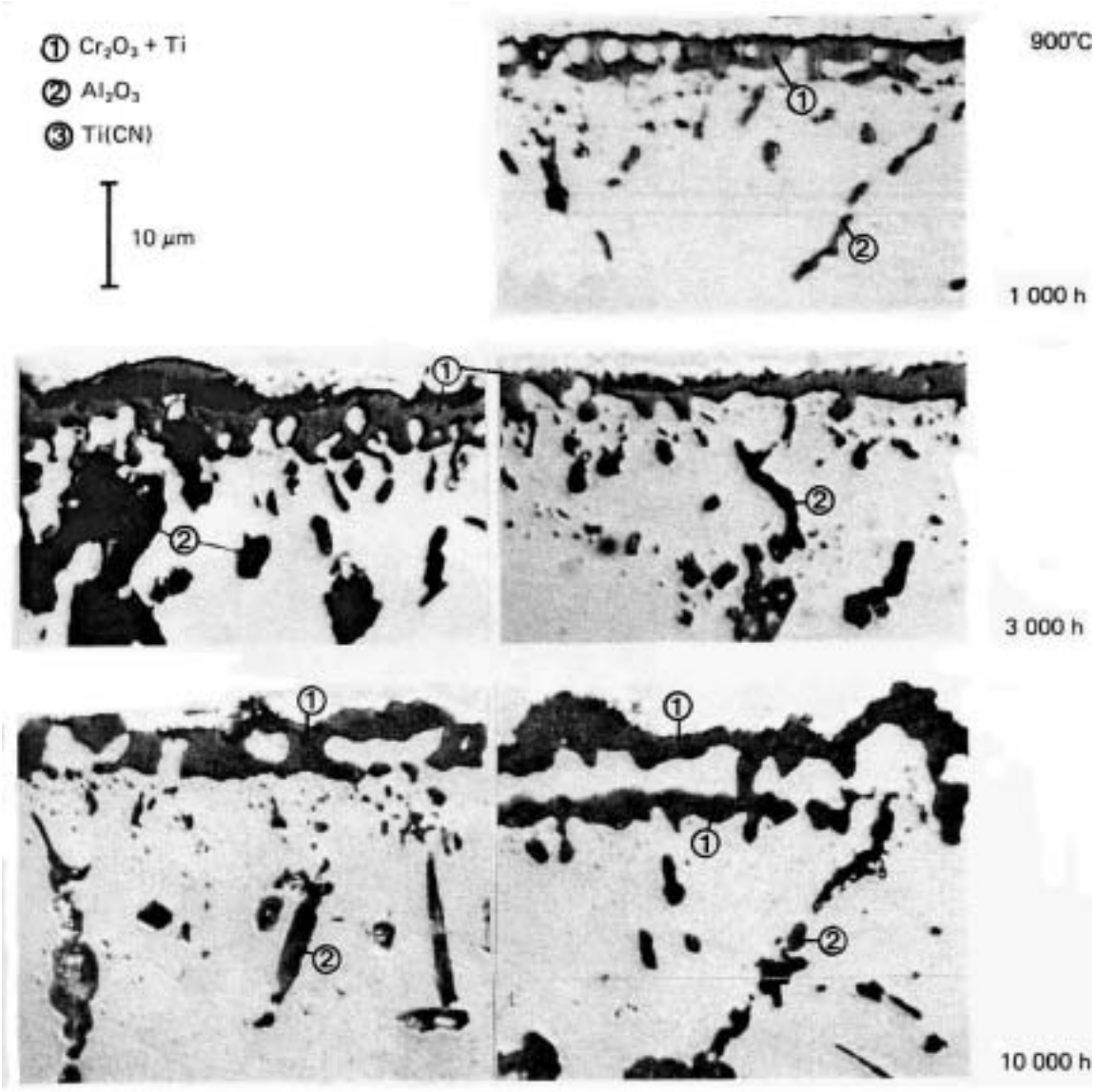

Figure 15

Evolution of chromium and manganese depletions by an evaporation phenomenon for Hastelloy X and XR after 1000 hours in helium at different temperatures (from (16))

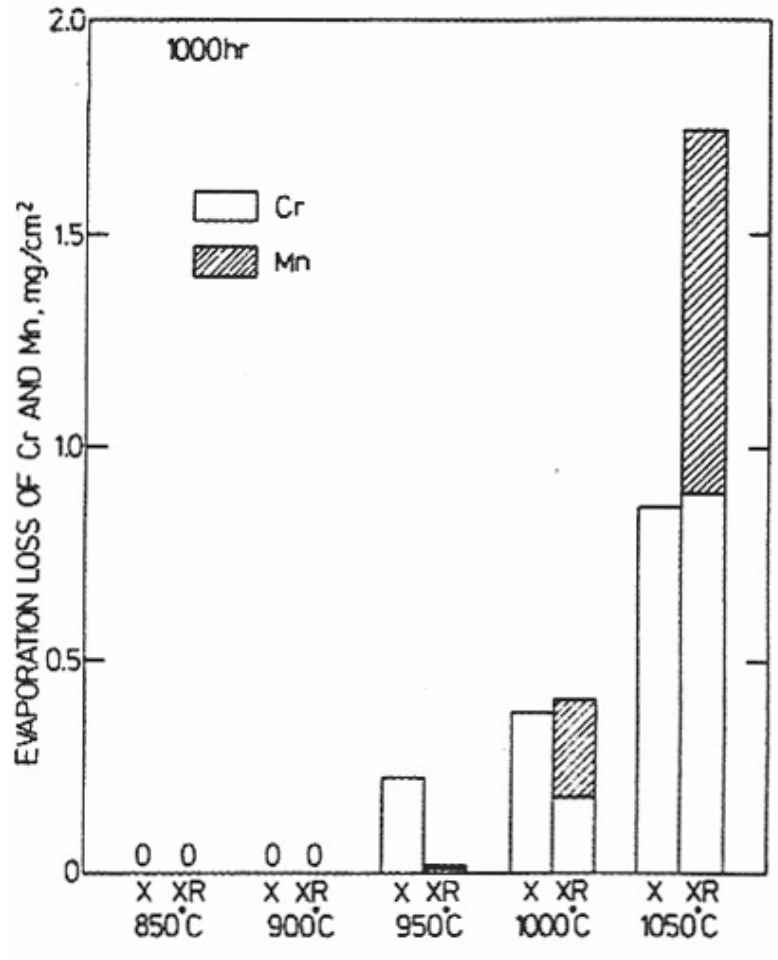

Figure 16

Whiskers due to evaporation phenomenon on the Hastelloy X at high temperatures: 1000°C and 1050°C (from (16))

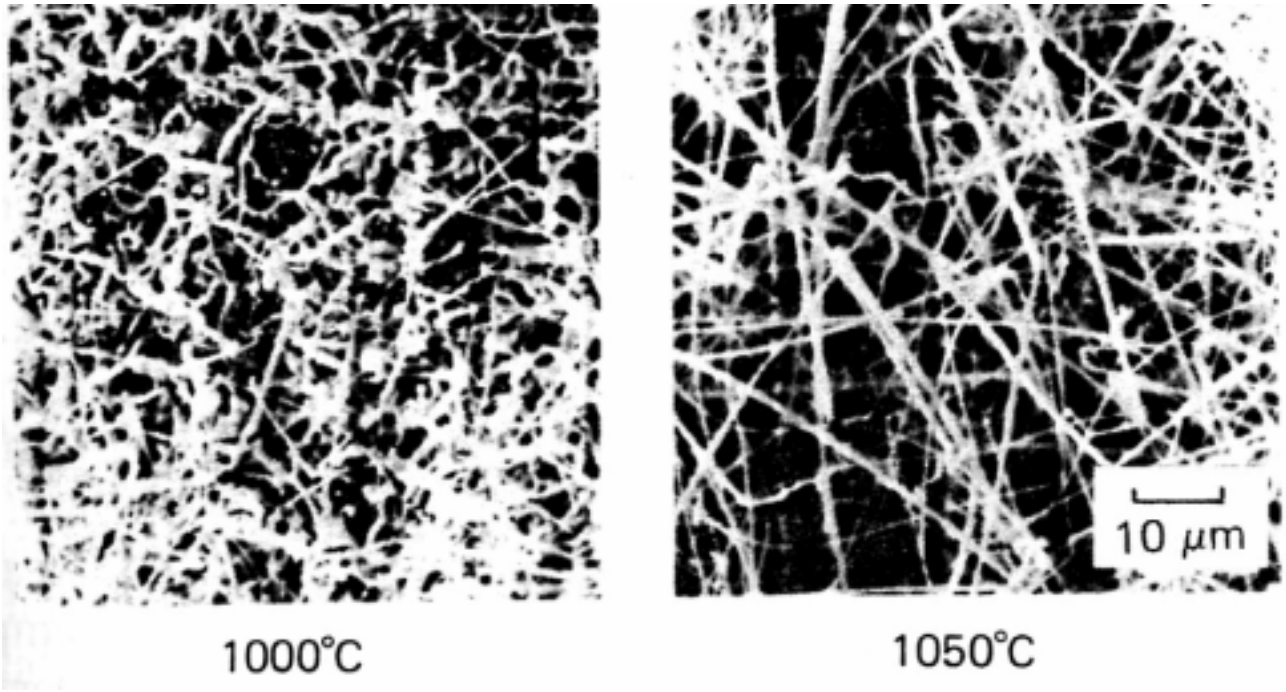

Figure 17

Spallation evolution as a function of duration for Hastelloy X and XR in a 1000°C helium atmosphere (from (16))

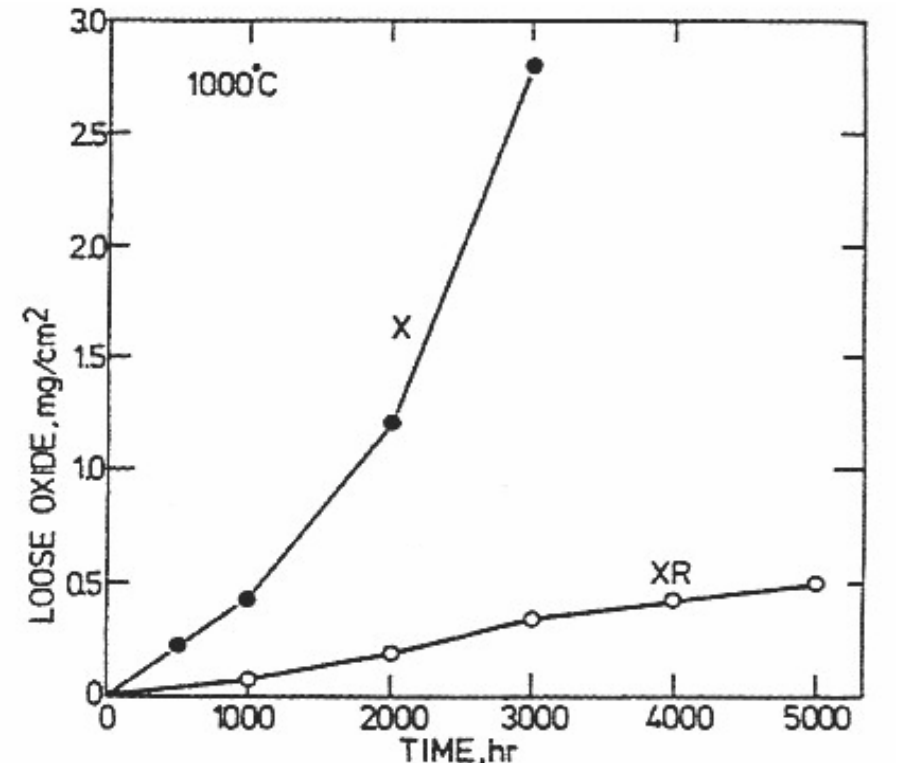

Figure 18

Chromium profile evolution with time of exposure in a 950°C helium atmosphere (H_2: 500µbar ; H_2O: 1,5 µbar ; CO: 100 µbar ; CH_4: 10 µbar) (from(37))

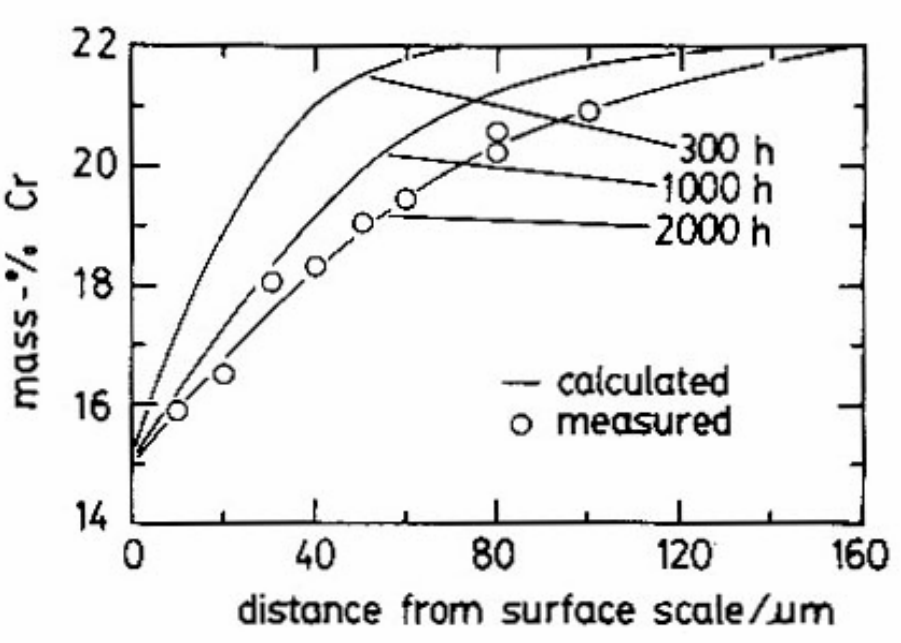

Figure 19

Alloy 617 in a 950°C PNP helium atmosphere: thickness evolution of the oxide scale and the internal oxidation depth, of the depth of carbide free zone and carbon pick up (from (38))

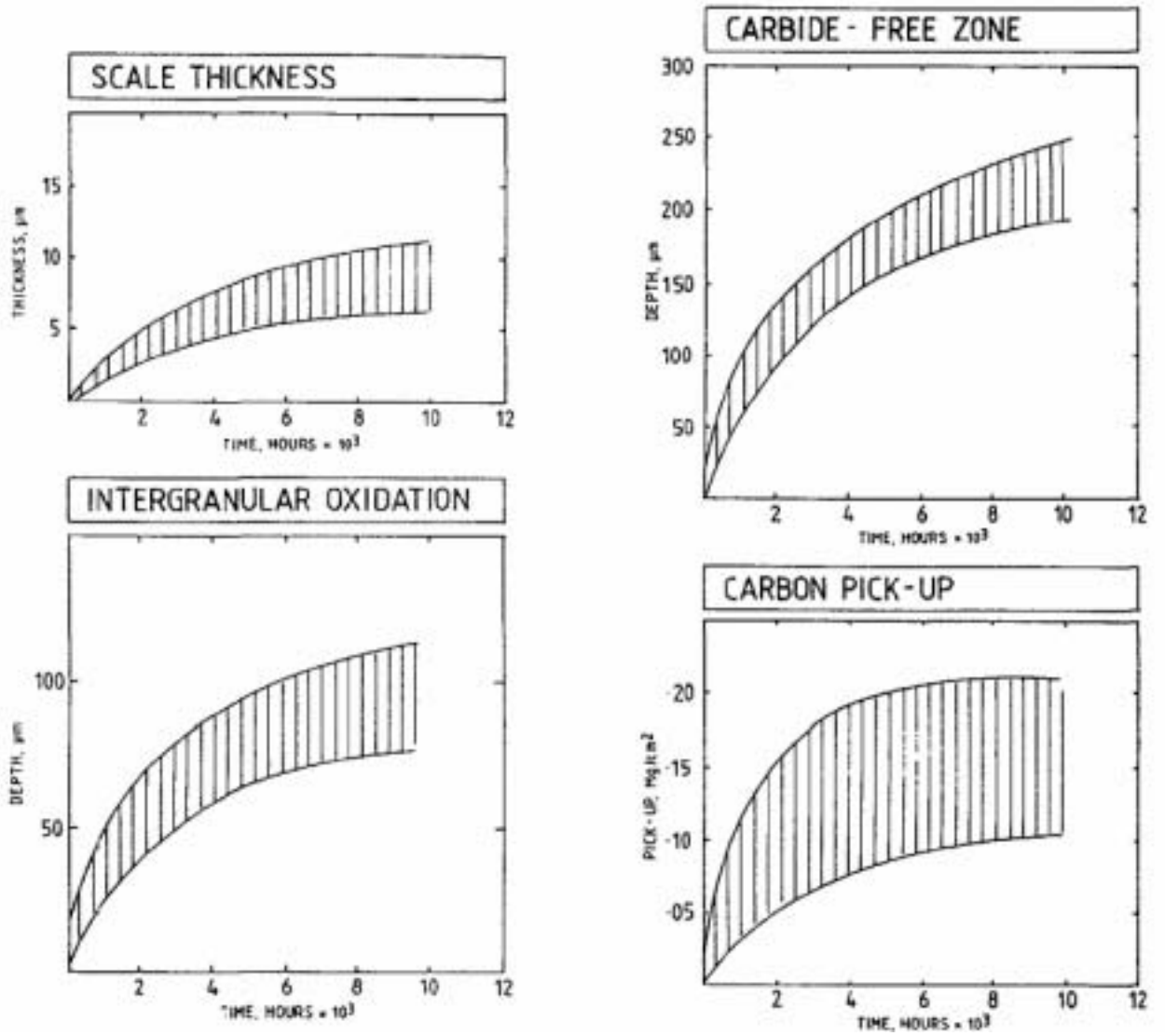

Figure 20

Evolution of the microclimate CO critical pressure P_{CO}* as a function of the temperature for 5 high temperature alloys (from(37))

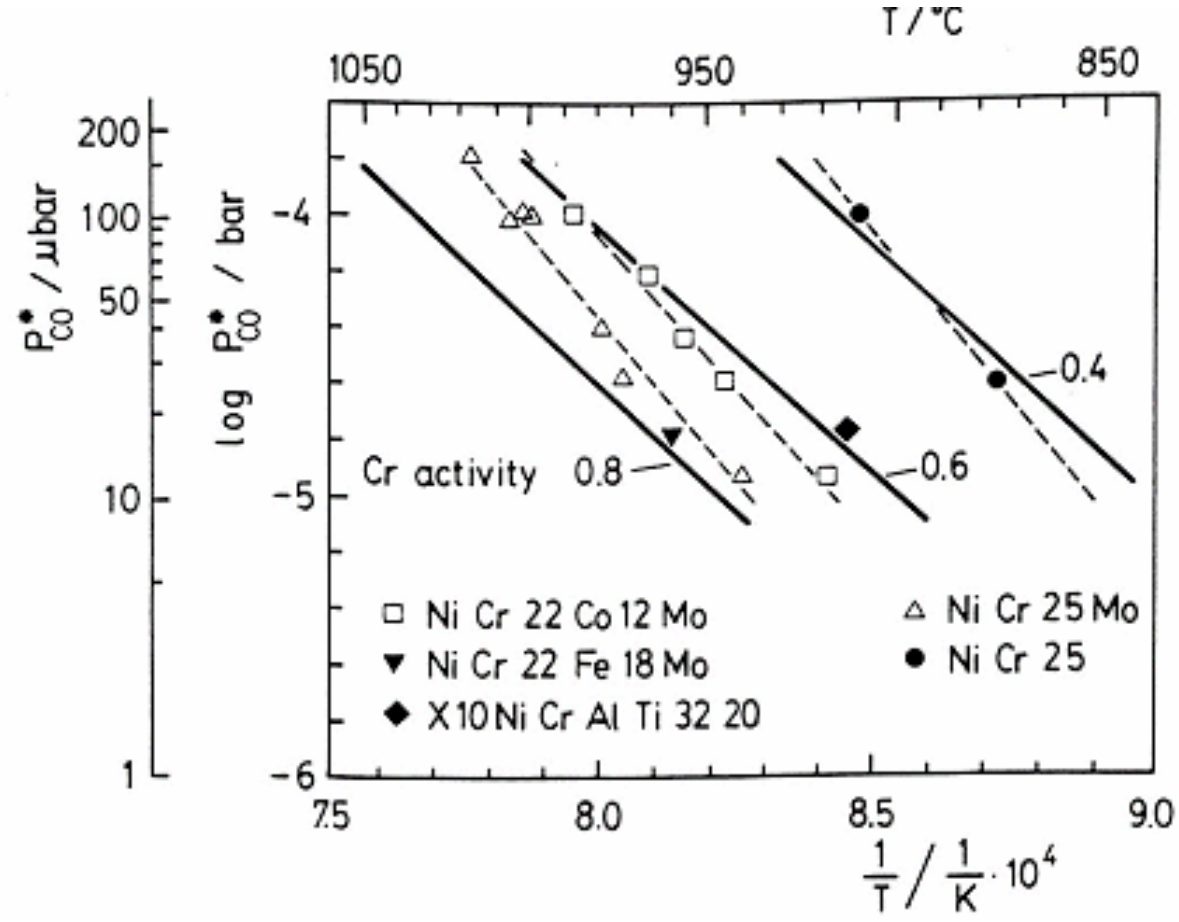

Figure 21

Calculated stability diagram of chromium at 950°C. Effect of the chromium activity and location of former HTR helium atmospheres

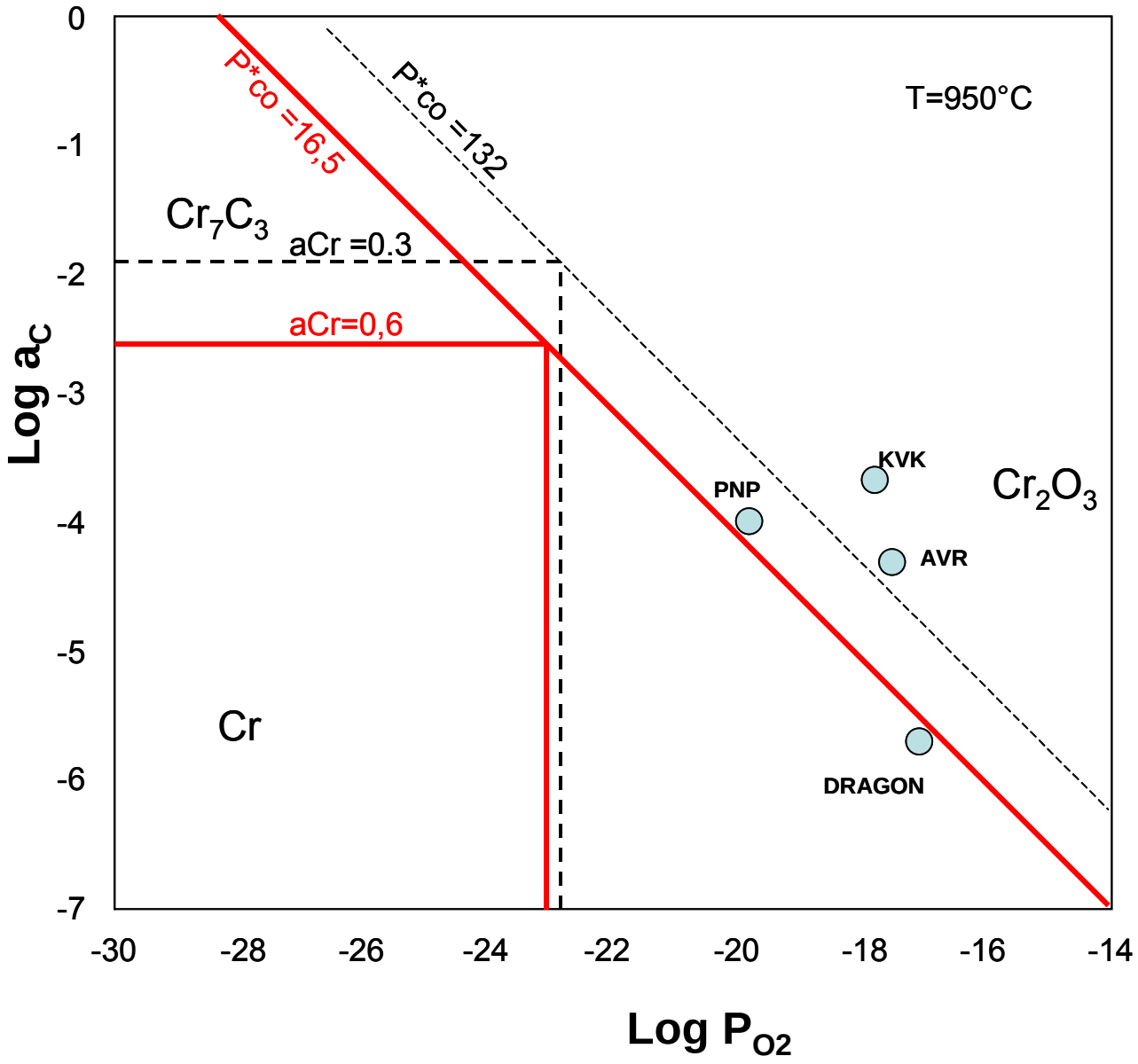

Figure 22

Calculated stability diagram of chromium at 1000°C. Effect of the chromium activity and location of former HTR helium atmospheres

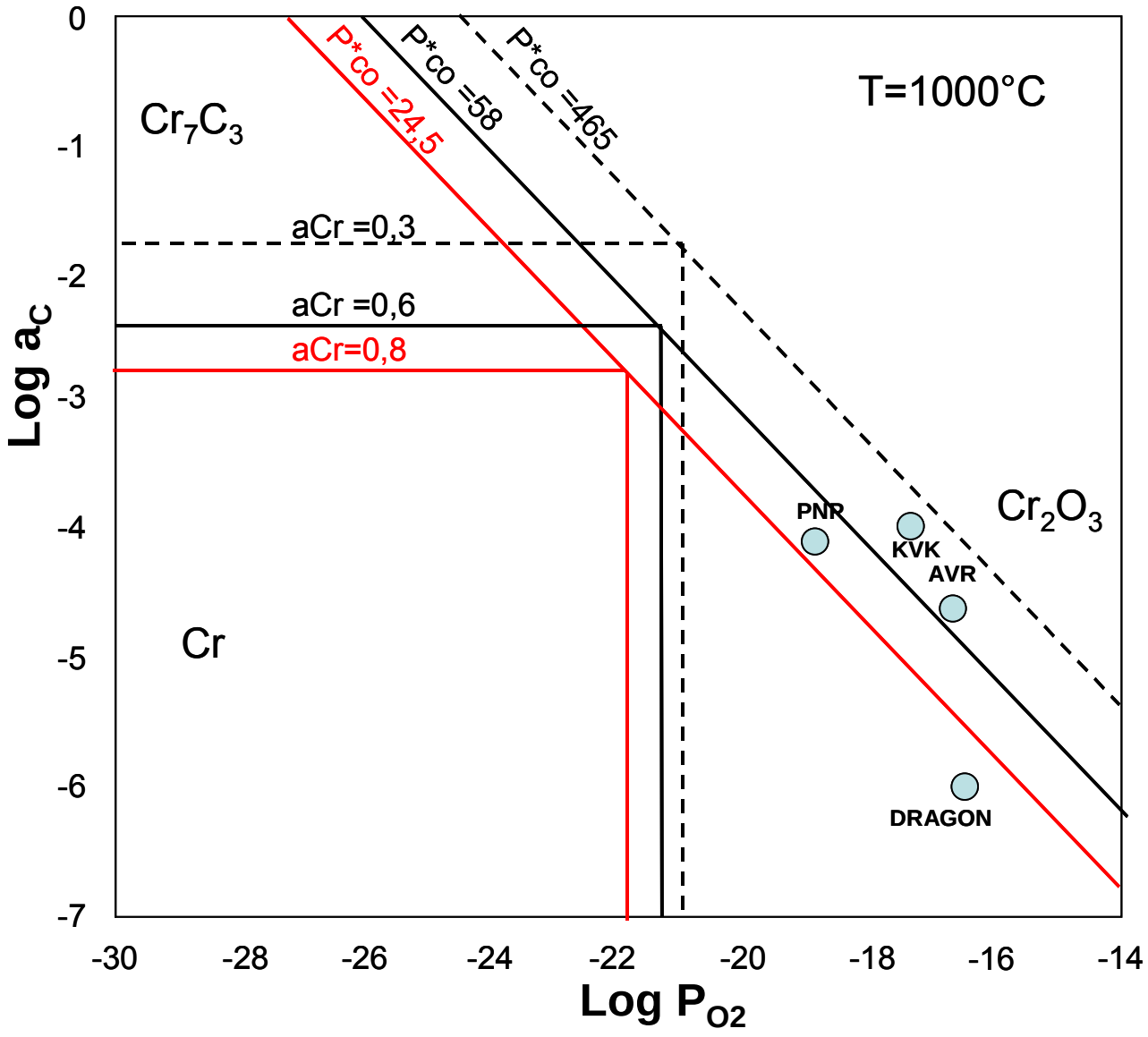

Table 1

Former helium environments

HTR facility	Helium composition (µbar)						
	H_2	H_2O	CO	CO_2	CH_4	N_2	Ref.
Peach Bottom	200	1	11	1	22	15	(10)
Dragon	10	1	8	0,5	1	12	(10)
AVR	500	1	2000	5	2	-	(10)
PNP	500 ± 50	1,5 ± 1	15 ± 5		20 ± 5	<5	(5)
THTR	135	1	2	50	40		(23)
HHT	50	5	5	50	5	5	(14)
KVK	200	6		240		300	(24)
HTGR-SC	200	10	1	20	20	15	(25)
HTR-GT	500	1	1	51	51	15	(25)
Jaeri typeB	200	1	2	100	5	5	(26)
Erans n°2	300	3	1	20	20	5	(26)
CIIR	500	1		35	40		(33)

Appendix 1

Stability diagrams and behaviour of Ni-Cr alloys

The behaviour of Ni-Cr alloys in HTR helium is primarily controlled by the Cr compounds which are stable in the relevant conditions, as they will determine the possible surface reactions leading to:

- metallic chromium, at low ac and P_{O2} levels,
- chromium oxide at high P_{O2} levels and
- chromium carbides at high a_C levels.

The domains of stability of these species are depicted on the phase stability diagram in figure A1-1.

In fact, the stability diagram is more complex since several chromium carbides may be stable. However, in the following discussion only one chromium carbide will be considered.

Seven different domains combining the different possibilities regarding the phase stability and the possible surface reactions have to be considered as regard the corrosion behaviour of Ni-Cr materials. The phase diagram in figure A1-1 shows these regions and summarises the corresponding behaviour of the Ni-Cr materials:

- In the region III-a, chromium oxide is stable ($P_{O_2} > P^S_{O_2}$). Thus, the formation of a protective layer on the alloy is possible. In addition, the carbon activity is in excess of the critical value for the formation of carbides ($a_C > a^S_C$). Thus, chromium carbides can be formed below the oxide, where the oxygen activity is low enough. Thus, both alloy oxidation and carburisation are possible, but, in many instances, the oxide film can limit the carburisation by limiting the access of carburising species to the metal surface. Provided that the oxide film is protective, **this region of the diagram is a safe region regarding the material degradation**, with light formation of carbides below the oxide layer.
- In the region III-b, chromium oxide is still stable but the carbon activity is too low for the chromium carbide to be stable. However, provided the pores of the oxide are not too large (which is the case for a protective oxide layers) the depletion of water in these pores causes a local increase of the carbon activity (due to the presence of CO) . As a consequence, the environment is slightly carburizing in the pores and the behaviour of the protective layer can be stable in the region III-b. According to Quadakkers, this region seems to be the safest.
- In the region IV-a, chromium carbide is stable and a non-protective surface layer of chromium carbides may be formed that allows internal carburisation of the material. However, at the carbide/alloy interface, the carbon activity is lower than in the bulk gas and, since $P_{O_2} > P^S_{O_2}$, a chromium oxide film may be formed below the carbide surface layer. However, this oxide is not very protective and cannot hinder further internal carburisation. Thus, this region is not safe for the Ni-Cr materials.
- In the region IV-b, carbon activity is high and carburisation may occur. If the porosity of the carbide surface layer is not too large, an oxide layer may be formed below the carbide layer due to a similar mechanism which have been described for the region III-b (local decrease of carbon activity to a^S_C and local increase of oxygen activity over $P^S_{O_2}$). In this case, the behaviour of the alloys are quite similar in regions IV-a and IV-b.
- In the region I, metallic chromium is stable, no protective layer can be formed and a strong decarburisation will occur.
- In the region II, chromium oxide is stable, but the low carbon activity will result in alloy decarburisation. Due to the gas evolution resulting from the decomposition of the carbides

the protective character of the oxide layer cannot be maintained .

It is worth noticing that the material may exhibit safe behaviour only if the partial pressure of carbon monoxide exceeds a critical value P^*_{CO}. Below this critical partial pressure no protective layer can be formed and the alloys exhibits severe damages either by carburisation or by oxidation and decarburisation. This corresponds to the "microclimate" reaction of Brenner . Below the critical partial pressure of CO, chromium oxide and carbide cannot coexist. If oxide are stable the decomposition of matrix carbide cause CO evolution which does not allow a compact oxide film to be maintained . If oxide is not stable, the base metal is not protected and severe carburisation or decarburisation occurs according to the carbon activity.

Oxygen and carbon activities

Quadakkers defines activities of oxygen and carbon in the helium gas as follows:

1. In the absence of methane

   - the activity of oxygen (expressed as P_{O2}) comes from the equilibrium of the reaction

$$O_2 + 2\ H_2 \leftrightarrow 2\ H_2O \text{ (18) .}$$

$$p_{O_2} = K_{18} \cdot \left(\frac{P_{H_2O}}{P_{H_2}}\right)^2 \text{ (19)}$$

   - the activity of the carbon comes from the equilibrium of the reaction:

$$CO + H_2 \leftrightarrow C + H_2O \text{ (20)}$$

$$a_c = K_{20} \cdot \frac{P_{CO} \cdot P_{H_2}}{P_{H_20}} \text{ (21)}$$

   - the carbon activity a_C can be written in the following form:

$$a_c = K_{18} \cdot \sqrt{K_{20}} \cdot \frac{P_{CO}}{\sqrt{P_{O_2}}} = \frac{1}{\sqrt{K_{23}}} \cdot \frac{P_{CO}}{\sqrt{P_{O_2}}} \text{ (22)}$$

     where K_{23} is the equilibrium constant of the reaction:

$$2\ C + O_2 \leftrightarrow 2\ CO \text{ (23)}$$

Thus, in helium, P_{O_2}, a_c and P_{CO} are not independent variables since they are bound by the relation (22). In addition a thermodynamic calculation shows that between 800 and 950° C the equilibrium partial pressures of CO_2 and CH_4 are negligible.

In the diagrams, the fact that P_{O_2}, a_C and P_{CO} are not independent variables implies that the point corresponding to a helium atmosphere lies on a oblique line corresponding to the partial pressure of CO in the environment.

2. In the presence of methane

If equilibrium would be reached, methane would completely decompose water according to the reaction

$$CH_4 + H_2O \rightarrow CO + 3\,H_2 \quad (24)$$

and the remaining methane would lead to the carburisation reaction:

$$CH_4 \rightarrow [C] + 2\,H_2 \quad (25)$$

This would yield to theoretical carbon activity far over 1 (actually values of the order of 10^3 can be calculated in some instances) which would lead to a strong carburisation potential with an effective carbon activity of 1.

In this case, the oxygen partial pressure which can still be related to the carbon activity through the relation (22) becomes (see the corresponding point on the diagram of the reaction):

$$P_{O_2} = \frac{1}{K_1}\left(P_{CO}\right)^2 \quad (26)$$

In fact, the reactions leading to methane decomposition are relatively slow and a better estimation of the carbon activity on the reacting surfaces can be obtained from kinetic arguments.

The border lines between region I and II is estimated by the equilibrium between chromium and its oxide. Its is established by the relation :

$$\frac{2}{3}\,Cr + H_2O \leftrightarrow \frac{1}{3}\,Cr_2O_3 + H_2 \quad (27)$$

The free energy change is given by ΔG^0=-RT ln K, where K is the equilibrium constant for the reaction. Thermodynamic database gives us the value of ΔG0 for a temperature T.

$$K = \frac{PH_2}{PH_2O.a_{Cr}^{1/3}} \quad \textbf{(28)}$$

So for a given chromium activity a_{Cr}, it is possible to established the ratio between P_{H2O} and P_{H2}.

The border line between region I and V is given by the reaction:

$$\frac{7}{3}\,Cr + C \leftrightarrow \frac{1}{3}\,Cr_7C_3 \quad (29)$$

We assume for this example that Cr_7C_3 is the concerned form of chromium carbide. Then the following relation allows to calculate the microclimate critical pressure (PCO*):

$$3\,Cr + CO \leftrightarrow \frac{1}{3}\,C_3Cr_7 + \frac{1}{3}\,Cr_2O_3 \quad (30)$$

We can so calculate the stability diagram for several kinds of alloys defined by their chromium activity for a given temperature. Nevertheless, when experimental data are unavailable, only results for theoretical alloys (parametric a_C) can be obtained.

Figure A1-1

Stability diagram of chromium

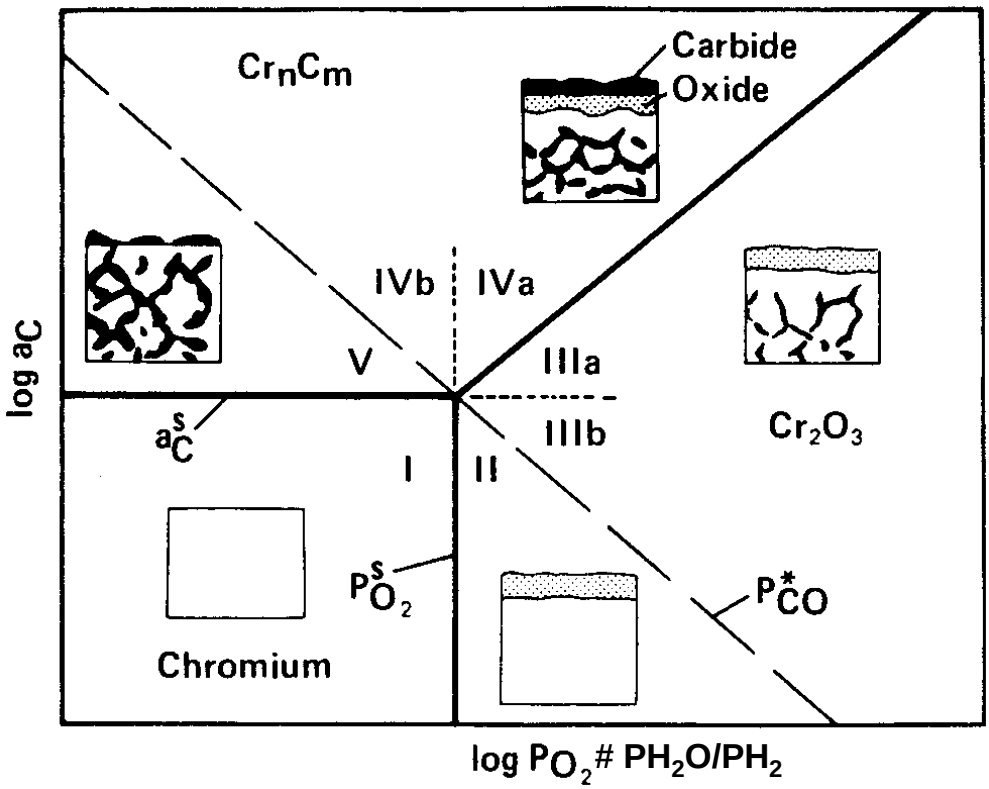

Appendix 2

Specificity of direct-cycle HTR - GT-MHR requirements

Nominal operation conditions of the GT-MHR primary circuit are:

- Pressure 7,1 MPa
- Temperature 490°C at core inlet
  850°C average at core outlet

Under normal operation conditions, the helium purification system (HPS) should maintain the following levels of impurities in primary helium:

- H_2O < 2 vpm
- $CO_2 + CO$ < 6 vpm
- H_2 < 5 vpm
- N_2 < 25 vpm

The GT-MHR helium purification system (HPS) consists of two lines, with the equipment for helium cleaning up from chemical and radioactive impurities, heat exchange equipment, pipelines, valves, instrumentation sensors and means for purification blocks regeneration.

The equipment of one HPS line, with functions and temperature modes of operation, are given in table A2-1.

Primary helium is taken to the HPS from a delivery plenum of the high pressure compressor. Purified helium is returned to the low pressure compressor suction cavity.

Primary helium flow rate through the HPS is 0,5 kg/s. Radioactive impurities retention time (noble gases and iodine) is 3 days for short-lived nuclides and 40 days for long-lived ones (Xe^{133}, I^{131}).

Helium flow through the filter for purification from long-lived radioactive substances is 10% of the total flow through the HPS.

Table A2-1

GT-MHR : main equipments of one HPS line

Equipment name	Function mode	Temperature
1. Pipelines for helium delivery from primary circuit compressor outlet and valves	Helium delivery to purification system	108°C
2. Heater	Helium heating before copper-oxide reactor	250-300°C
3. Copper-oxide reactor	Removal of H_2, CO, CO_2 impurities	250-300°C
4. Recuperator	Heating of helium returned to the primary circuit	350-400°C
5. Heat exchanger	Helium temperature decrease	from 350-400°C to 35°C
6. Cooler	Helium cooling	from 35°C to 10°C*
7. Moisture separator	Moisture removal	10°C
8. Coal adsorbers	Activity supperssion of noble gases and iodines short living isotopes	Compartment temperature
9. Mechanical lifter	Protection against dust	Compartment temperature
10. Zeolite absorber (one is operating and the other regenerated)	Removal of CO_2 impurities and HO_2 is steam**	Compartment temperature
11 Mechanical filter	Protection against dust	Compartment temperature
12 Coal absorber	Activity supperession of noble gases long-living isotopes	Compartment temperature
13 Startup compressor***	Provision of before startup prim. circuit purification	Compartment temperature
14 Pipelines for helium return to primary circuit compressor inlet and valves	Helium delivery from purification system to the primary circuit	300°C